Step Growth of Two Flexible $\mathbf{AB}_f$ Monomers: The Self-Return of Random Branching Walks Eventually Frustrates Fractal Formation

Colin Cameron,[†] Allan H. Fawcett,[*,‡] Cecil R. Hetherington,[‡] Richard A. W. Mee,[‡] and Frederick V. McBride[§]

Courtaulds Coatings, Stoneygate Lane, Felling, Gateshead, NE10 OJY, England, U.K.; School of Chemistry, and Computing Services, The Queen's University of Belfast, BT9 5AG, Northern Ireland, U.K.

Received September 21, 1999; Revised Manuscript Received April 11, 2000

ABSTRACT: The competition between the growth of hyperbranched structures and cycle formation that occurs when flexible $\mathbf{AB}_f$ monomers undergo step growth has been simulated with a three-dimensional lattice model in which the monomers are mapped onto several lattice sites. To explore the effect of functionality we have performed studies with $f = 2$ and 4. The growth is initially fractal, for molecules and branches are self-similar, but it becomes controlled by the formation of intramolecular bonds, a possibility enhanced by growth, for the **A** group at the root of the growing Cayley tree might react with one of the **B** groups on the tips of the developing branches. Ultimately every molecule contains a cycle. At $t = \infty$ the most likely cycle has $m = 1$ residue, with $\langle m \rangle_{n,\infty} = 1.65$ for the $f = 2$ system and 1.39 for the $f = 4$ system, and the corresponding values of the degree of polymerization, $\langle x \rangle_{n,\infty}$, are 10.7 and 7.5. Whatever the value of f, the incidence of cycles throughout the reaction of the two $\mathbf{AB}_f$ monomers follows the relationships $R_m = C_o\, p_a^m\, m^{-\gamma_1}$, with p_a the extent of reaction. γ_1, being 2.714(±0.005) for the $\mathbf{AB}_2$ system, and $C_o = N_o \langle x \rangle_{n,\infty} / \zeta(2.714)$, where N_o is the initial number of monomers. The mean degree of polymerization is given exactly by $\langle x \rangle_n = 1/(1 - p_e)$, where p_e includes only the extent of reaction between the molecules. The number of oligomers of size x follows the Flory distribution expression just to start with, and later only if the expedient is adopted of replacing p_a with p_e, but at the end—when $f = 2$—a second power series is found: $N_x = N_{1,\infty}\, x^{-1.5}$ for $0 < x < 48$. The exponent, $-\chi_w$, in the corresponding weight distribution function is −0.50, a value that cannot persist to high values of x, since the sum of that series is not bounded, so N_x and W_x must fall faster at higher x. These power laws are independent of the manner in which the $\mathbf{AB}_2$ molecule is mapped onto the lattice. In the $\mathbf{AB}_4$ system again rings form, but both their distribution at moderate values of m and the number and weight distributions, N_x and W_x, are curved on the double logarithmic plots, and are so even at the end for N_x and W_x when $x > 12$. The initial values of γ_1 and of χ_n are 2.8 and 1.29 respectively, and measure the greater ease of cycle formation and of scope for growth when $f = 4$. The eventual deviation from the early trends may reflect the exclusion from the neighborhood of the **A** groups at the roots of trees of other fractals, thus promoting cyclizations intramolecularly, and it occurs sooner, as m or x rises, when f is doubled. The populations of all the structural isomers among the lower oligomers have been obtained for both systems, and the extra isomers among the $\mathbf{AB}_4$ oligomers identified. Mean extent of reaction vectors and Kirchhoff matrices were obtained for these and the higher oligomers, so that the patterns of molecular structure are demonstrated in both systems at three stages of the reaction: some structural characteristics are similar as in fractals, as the size varies. The molecules grow as hyperbranches, but as they flourish a route is eventualy found back to the **A** group at the tree, so terminating growth and limiting objects to a finite size.

Introduction

It has been usual, when considering the step growth reactions of monomers of the type $\mathbf{AB}_f$, to expect the products to be hyperbranched molecules of infinite molecular weight and to follow Flory[1,2] in neglecting the formation of cycles,[3−6] as in early models of gelation.[1,2,7,8] The molecules have the topology of a Cayley tree[9] and are produced by a type of growth that is entirely fractal in nature,[10] since they and their branches are self-similar in the mean: all along at each step growth what becomes a branch was formerly one of the trees. Cycles have also been neglected when considering[6,11] the recently introduced self-condensing vinyl polymerization reaction,[12] which resembles the $\mathbf{AB}_2$ case, an omission that may be appropriate to the monomer as the reactive sites are on opposite sites of an aromatic ring but may not be suitable within all of the oligomers. Despite the relative simplicity of the expressions that are provided by this approach and the scope for its development,[5,6] it is difficult to ignore the possibility of the formation of cycles within the elaborate and high molecular weight structures that are resplendent with functional groups, if they are not stiff. The stoichiometry of the molecule would certainly allow cyclization, for at the root of each tree there always lies one **A** group, and the larger the degree of polymerization achieved, the more **B** groups there are for it to react with intramolecularly. All that is required is that the **A** and **B** groups might approach each other in space, something that is readily realized in our simulations on a lattice,[13−17] which thus allows us to develop a new paradigm for the polymerization of flexible $\mathbf{AB}_f$ systems in three dimensions.

A classical description of the configuration of a linear polymer chain has been the nonreturning random walk, an idea that was explored by simulating the growth of a chain on a lattice, as in an athermal medium, prior

* Author for correspondence.
† Courtaulds Coatings.
‡ School of Chemistry, The Queen's University of Belfast.
§ Computing Services, The Queen's University of Belfast.

10.1021/ma9916032 CCC: $19.00
Published on Web 08/01/2000

to studying its configurations.[18−20] Obtaining samples of long chains by this method was extremely difficult, for there was found to be an accumulative attrition caused by the possibility that the latest additional bead might be placed on a site that had already been taken[20]—an event that would break the nonreturning condition. These studies point to an expectation of cycles in step-growth polymerizations. In the present case there are differences in detail, for we form the polymers by step growth of molecules already upon the lattice rather than by adding an extra bead—the excluded volume condition is satisfied a priori. Moreover the molecule becomes hyperbranched, as each residue may react more than twice, so the chances are enhanced that a path might form back to the single bead at the root of the tree. Furthermore, we have obtained some evidence that chains produced by step-growth become more compact in their configurations as the medium reaches a higher molecular weight and Θ-conditions are approached, a factor which may enhance cyclization.[14,21] By giving proper respect to the manner in which molecules occupy space, the lattice representation does not allow the formation of isomers that would have impossible packing problems around their exteriors.[22] From all those trees that may be generated by Pólya's theorem[1,23,24] and the graphs (the structures formed by cyclizations) the simulation selects just those that might realistically form, and readily discovers the structural isomers and their proportions produced when following the rules of the chemical reaction. The 26-choice bonding pattern around each lattice site appears to have ensured in previous studies an insensitivity of certain results to the structure of the lattice itself,[13−17] a statistical property we attribute to the group chemical functionality being much smaller than the lattice coordination number. That corresponds well to real chemical systems. This method for simulating polymer chemistry avoids using a series of differential equations for each possible reaction that might be envisaged between each site of every possible structural isomer,[25] a requirement that would place an impossible demand upon the computer for achieving a complete reaction. It lies between the off-space or infinite dimensional "graph models" of structural growth and the percolation lattice models[26] and produces trees and graphs that are properly embedded in and move[17,27] within three-dimensional space.

Previously we have shown that cycles do form from the evolving trees of a model $\mathbf{AB}_2$ system, and that their formation creates a limit to the growth of the molecules by consuming a proportion of the **A** groups in a nonpolymerizing side reaction.[17] Since the preliminary account appeared of our Monte Carlo studies of such reactions on a lattice,[28] we have learned of experimental evidence for cycles in $\mathbf{AB}_f$ polymerizations: they have been directly detected by NMR spectroscopy in a hydrosilane/olefin system,[29] whose reported inability to reach infinite size[30] informed and stimulated our work. In a related system NMR spectroscopy has found the monomeric species to be cyclized at the end of the reaction,[31] and elsewhere the absence of **A** groups has been noticed.[32] It has also been disclosed that cycles form in certain polyester systems, where stiff aromatic nuclei of the $\mathbf{AB}_2$ monomers cause the predominant cycles to be the trimers,[33] according to a mass spectroscopic analysis of the final products. Thus, some of the predictions of our approach[28] have quickly been supported by these experiments, which also bear out certain experiences within the paint industry on the ton scale. However, if the stiff component of the monomer is not supplemented,[34] as Feast arranged,[33] by a flexible component, or if the second **B** center is deactivated when the first reacts, as with poly(aramids),[35] then the formation of cycles may indeed be impossible, at least within the oligomers. As $\mathbf{AB}_f$ systems offer a cheap one-pot route to the formation of randomly hyperbranched molecules that resemble the regular starburst dendrimers[22,32,34,36−40] and have interesting solubility and viscoelastic properties, our results may be of some value.

After monomers of the standard **AB** step growth type, those of the $\mathbf{AB}_2$ form are the next more elaborate, and the $\mathbf{AB}_4$ types are yet more functional, being capable of producing more higly branched dendrimers, and probably more readily capable of cyclization. The competition between growth and cyclization that is present in this polymerization, and which intensifies as f rises, is there also in network formation but here the products are of a finite size, and so are more readily analyzed. As we show in essence in Figure 1, Cayley trees develop, and each becomes a graph when a cycle forms. Here we examine the formation from two $\mathbf{AB}_f$ monomers of self-returning random branching walks and the structures that precede and then flourish around them as the **A** and **B** groups link together. We wish to discover how the mean size of the self-returning walks, $\langle m \rangle_n$, the mean degree of polymerization $\langle x \rangle_n$, other measurements of molecular size, the cycle and molecular weight distributions, and the proportion of different structural isomers of each size of molecule are varied during the course of the reaction and when we double the number of **B** functional groups in the monomer.

Our method of recognizing individual structural isomers with a set of node priority values[17] is extended to the extra isomers created from the $\mathbf{AB}_4$ monomers. In them there is the possibility of a residue containing a loop being linked directly to three further residues: at the $x = 3$ stage, there is one extra isomer, and for $x = 4$ and 6 there are respectively 2 and at least 20 more, though their occurrence requires the formation first of less elaborate precursors, so they are likely to be less frequent. A previous exploration used the following monomer: $\mathbf{A}-X-X-N(-\mathbf{B})_2$, the X beads producing flexibility and keeping the **A** and **B** group beads well apart. At the end of the polymerization it was found that the cycle distribution followed the terms in a Riemann ζ function, the argument, 2.710(±0.007), being interestingly close to e, and that the number of oligomers of size x following $x^{-1.5}$, i.e., the terms of $\zeta(1.5)$.[17] These distribution functions naturally differ from the Flory expressions[1] (whose derivation ignored cyclization), and are so simple that we wish to discover how general they are. Are they to be found when the spacers X are absent in the simplest $\mathbf{A}-N(-\mathbf{B})_f$ lattice representation, and when both branching and cyclization is easier ($f = 4$), as with the molecules of the present study?

The Model

For this polymerization of two $\mathbf{A}-N(-\mathbf{B})_f$ monomers ($f = 2, 4$) we place each functional group and the node, N, of the molecule on adjacent lattice sites, linking them together by bonds of length l and $\sqrt{2}l$ in two-dimensional layers. After movements bonds of length $\sqrt{3}l$ appear in the 26-choice scheme.[13−17] This was designed to circumvent the problems encountered on a simple cubic lattice.[41] The lattice-based bond corresponds to

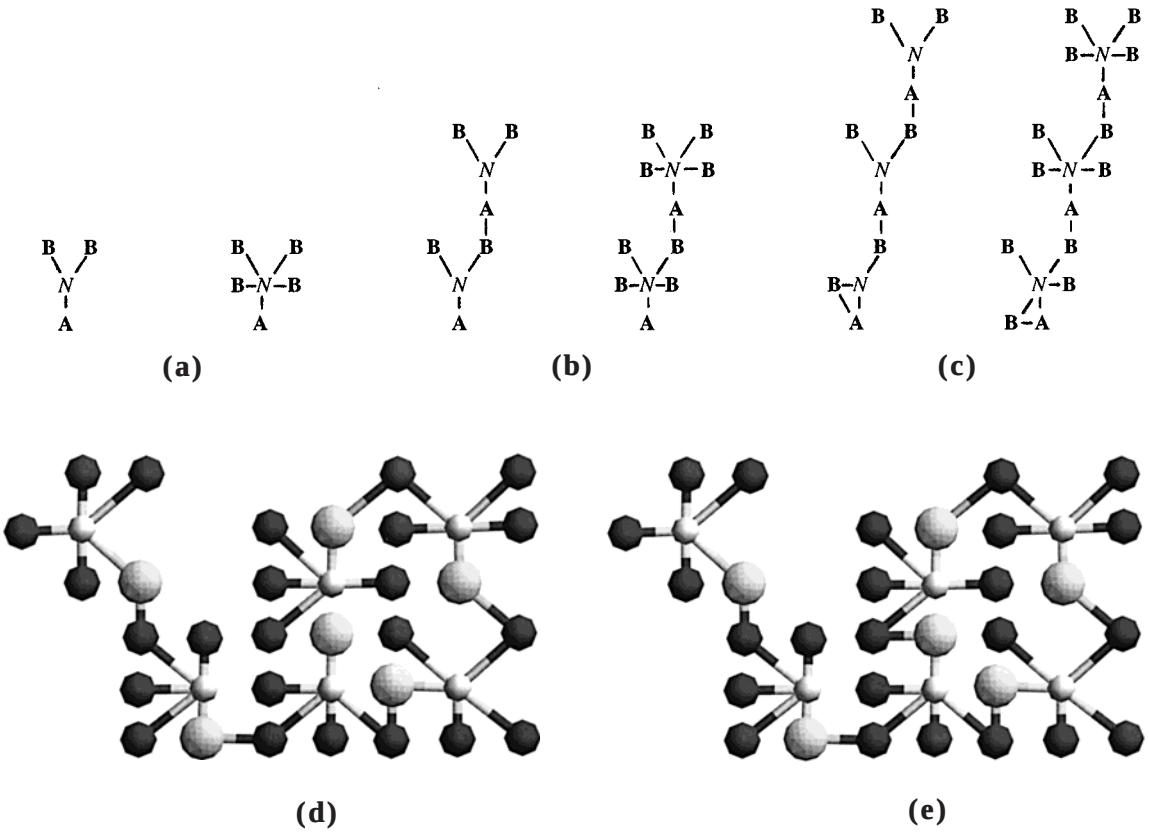

Figure 1. $\mathbf{AB}_2$ and $\mathbf{AB}_4$ monomers (a), the growth of Cayley trees (b), and their cyclization to yield a graph (c) in a two-dimensional display. Each **A** and **B** functional group and each node, *N*, occupies a lattice site. Here we show only the **B** groups moving. It may be seen that the scope for branching and for cycle formation are both greater in the latter case. We show a typical oligomer with $f = 4$ in two dimensions in part d, where the unreacted **A** root of the tree may react with a **B** group on the same residue, on the neighboring residue, or one of two **B** groups on a more remote residue. (e) Hexamer after the formation of a four-node cycle. (The simulation ran in three dimensions.)

several covalent bonds in a real molecule[14,17,42−44] and, in a coarse-grained manner, neglects the well-known details of the rotational isomeric state approximation[45,46] and also omits any expression of stiffness, both within the monomer and at the newly formed bonds: by allowing all possible lattice angles we have a type of fluctuating bond model[14,17,42−44,47] which explores chemical change. A comparison of the results of the present $\mathbf{A}-N(-\mathbf{B})_2$, simulation with those of the earlier $\mathbf{A}-X-X-N(-\mathbf{B})_2$, study[17] will allow, however, a crude effect of the mean distance between **A** and **B** groups within a monomer, $\langle b^2 \rangle$, to be appreciated. Each monomer was placed within a simple tiling pattern in one of a small number of configurations on a block of four or six lattice sites, each row of tiles being staggered with respect to one of its neighbors. Here, 10% of the sites were left free, in initial blocks of four or six, to represent free volume. The movement scheme for a single bead has already been described in detail;[17,27] the essential feature is that each bead may move to another site provided that it remains bonded to its companions in the same molecule. Just as it may exchange positions with beads of other molecules, the bead may exchange positions with other beads within the same molecule, whether they are adjacent or remote in the molecular framework. As movements accumulate, so a molecule rotates and diffuses.[42] Selection from the set of possible moves was made randomly, the choices being weighted with 0.5^q, where q was the number of bonds to be moved, to reflect crudely the ease of movement of end and pendant groups. So, while nodes might move, it is the **A** and **B** groups, which we sought to involve in chemical reactions, that enjoyed the greatest freedom. The monomers were subject to a number of these movements to randomize their initial orientation and position from the 2-D arrangement,[48,49] and to disperse the free volume. Except for the representations of the molecules upon the lattice the studies followed similar lines to that previously reported.[17]

The reaction proceeded by attempting at every CHOICE cycle (the unit of time) the random linking of pairs of adjacent **AB** groups, followed by 5 ($f = 2$) or 10 ($f = 4$) randomly dispersed attempts at movements, a process that prevented an **A** group being completely isolated all the time. All **B** groups had the same reactivity, irrespective of their location or any previous reactions in the same residue. It was unlikely that an **A** group would be unable to react, as an excess of **B** groups persisted throughout the polymerization. The Monte Carlo technique is ideal for establishing the elusive pattern of behavior created by a set of such involved rules as apply here.[50,51] To obtain a representative of the reaction, we used a 60^3 lattice system with periodic boundaries, and performed 9 ($f = 2$) or 10 ($f = 4$) repeats, storing the records on the structure of the system at several stages during the reaction. The program itself was written in PASCAL.[14,17,49] An analysis program then was used to appraise the changes brought about by the Monte Carlo evolution.[49]

Results and Discussion

(A) General Considerations. As the polymerization proceeded by a random selection of sites for attempting

Table 1. Power Laws for the Cycle Distribution Functions in the A−N(−B)$_f$ Systems Obtained by Fitting Eqs 3 and 4 to the Points of Figure 3[a]

f	m	$C_{m'}$	m'	C_m	no. of points
2	1	3563.6(±2.9)	0.996(±0.003)	3565.3(±2.6)	11
2	2	584.9(±1.2)	2.16 (±0.02)	572.0(±6.7)	11
2	3	183.8(±0.8)	3.24 (±0.03)	180.0(±1.9)	11
2	4	86.3(±0.4)	4.25 (±0.06)	84.4(±1.7)	7
2	5	40.9(±0.9)	5.13 (±0.14)	40.2(±0.6)	7
4	1	3557.3(±6.3)	1.015(±0.003)	3536.9(±9.1)	13
4	2	517.1(±1.5)	2.07 (±0.01)	513.2(±2.8)	10
4	3	147.6(±0.7)	3.10 (±0.03)	147.1(±0.6)	10
4	4	53.7(±0.6)	3.87 (±0.06)	54.4(±0.6)	9
4	5	24.2(±0.1)	4.93 (±0.04)	24.3(±0.1)	7

[a] There were N_o = 48 603.0 **A**−N(−**B**)$_2$ monomers initially present (ideally 48 600), f = 2: p_a was 0.999 97 after 5M CHOICE cycles. In the second study 32 454.4 **A**−N(−**B**)$_4$ monomers were initially present (ideally 32 400), f = 4: p_a was 0.999 74 (±0.000 03) after 2M CHOICE cycles (1M = 10^6).

a reaction, the initial rate of linking together **A** and **B** groups diminished greatly, but movements were maintained at a fairly constant rate. The movement attempts succeeded more than 60% of the time, decreasing from 83% to 74% for the **AB**$_2$ system and from 82% to 63% for the **AB**$_4$ system as the **A** and **B** groups reacted to form more-constrained segments. The present lattice model thus allows movements in the bulk more readily than did the early simple cubic lattice model for the isolated chain.[52,53] The polymerizations were run for a sufficient number of CHOICE cycles to allow the reaction of more than 99.9% of the **A** groups initially present, 5M cycles being used for the **AB**$_2$ monomer and 2M cycles for the **AB**$_4$ monomer, which was found to react more quickly (see footnote to Table 1). On a logarithmic time scale sigmoidal plots of the extent of reaction of the **A** groups were obtained, as noticed before.[13,17]

In the constitutional equation[13,17]

$$N_b + N_t = N_o + N_c \tag{1}$$

N_o is the number of molecules initially present, and, at time t, N_b is the number of bonds that have formed, N_t is the number of molecules present, and N_c is the number of cycles. It may be seen that when a ring or cycle forms, N_c and N_b each increment by one, so the extent of reaction rises, but N_t does not change. We have admitted cycles to eq 1, to recognize their possibility; once cycles are allowed, their incidence is left in the hands of the random processes within the fluctuating system (for *we* know of no *demon* capable of intervening in a real polymerization).[54] It may readily be seen that as the reaction proceeds and N_b tends to N_o, then N_t must finally become N_c. The Carothers function[1] may be derived from eq 1 by neglecting N_c, but the simulation allows cycles in an unbiased manner, and so behaves as may a real system. The present simulations do find that for both systems N_t does indeed tend toward N_c, the values at the end of the two studies being equal (N_t/N_o = 0.093 30(±0.000 30), N_c/N_o = 0.093 27(±0.000 46), f = 2, and N_t/N_o = 0.133 68(±0.000 66), N_c/N_o = 0.133 37(±0.000 90), f = 4), except for trivial discrepancies reflecting the fact that p_a did not quite reach 1.000 00.

(B) Cycle Formation. In the number fraction of molecules containing cycles, $F_{n,c}$, the denominator becomes smaller as the trees link together, link to a graph, or occasionally change to a graph, and the numerator rises as it counts these latter infrequent events. The plots in Figure 2 confirm that as the reaction proceeds this fraction rises for both systems toward unity. Both curves pass the 50% mark after p_a = 0.89, the **AB**$_4$ system leading the way, showing that in it cyclization is easier. If we divide eq 1 by N_t, we obtain

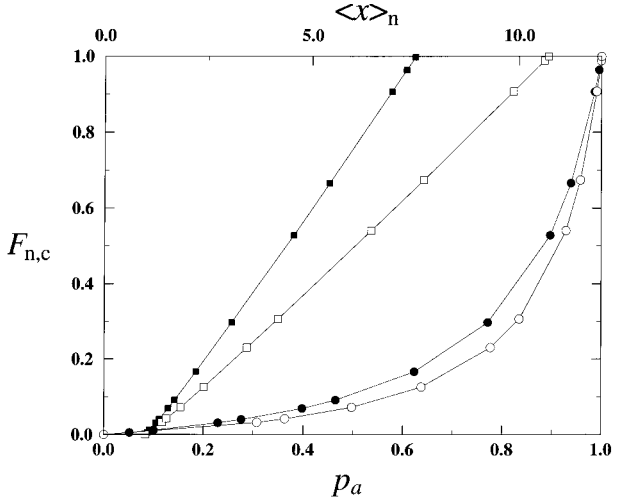

Figure 2. Plots of the number fraction of molecules that contain a cycle, $F_{n,c}$, against the extent of reaction of the **A** groups, p_a (circles), and against the mean degree of polymerization, $\langle x \rangle_n$ (squares). The symbols are open for the **AB**$_2$ system, and filled for the **AB**$_4$ system.

$$N_b/N_t + 1 = \langle x \rangle_n + F_{n,c} \tag{2}$$

Now, as t moves from 0 to ∞, N_b/N_t changes from 0 (or $0/N_o$) to $N_o/N_\infty = \langle x \rangle_{n,\infty}$, and so $F_{n,c} = N_c/N_t = N_c/(N_{br} + N_c)$ must become unity (N_{br} includes branched and linear molecules). The slope of the plots of $F_{n,c}$ against $\langle x \rangle_n$ measures the relative proportions of cyclization and of growth reactions, and is smaller at the start, as then only loops can form. Consequently it is first a little smaller than, and finally a little larger than, the mean value, the reciprocal of $\langle x \rangle_{n,\infty} - 1$. If we ignore this slight drift in the slope, we may write $F_{n,c} \approx (\langle x \rangle_n - 1)/(\langle x \rangle_{n,\infty} - 1)$.

(C) Cycle Distributions. We have reported how R_m, the number of rings of size m in the first (**A**−N(−**B**)$_2$) system, varies as the reaction proceeds,[55] and show those results again, together with the results from the second (f = 4) model in Figure 3, parts a and b. The extent of reaction was obtained from N_b/N_o, the ratio of the number of bonds that formed to the number of molecules—or of **A** groups—initially present. It appears that cycles accumulate, small ones first and larger ones later, once their precursor oligomers have formed. In both **AB**$_f$ systems straight line relationships are obtained in these double logarithm plots of R_m against p_a. We have fitted the data with eq 3, with m' allowed to be noninteger

$$R_m = C_{m'}\, p_a^{\,m'} \tag{3}$$

and report the values of the constants $C_{m'}$ and m' in Table 1 for the two systems. The values of $C_{m'}$ and m' were obtained by a nonlinear least-squares fitting procedure[17,56] and for the present **AB**$_2$ case are not quite as close (in terms of the standard deviation) to integer values as they were for the more elaborate **A**−X−X−N(−**B**)$_2$ case,[17] perhaps because the present range of p_a

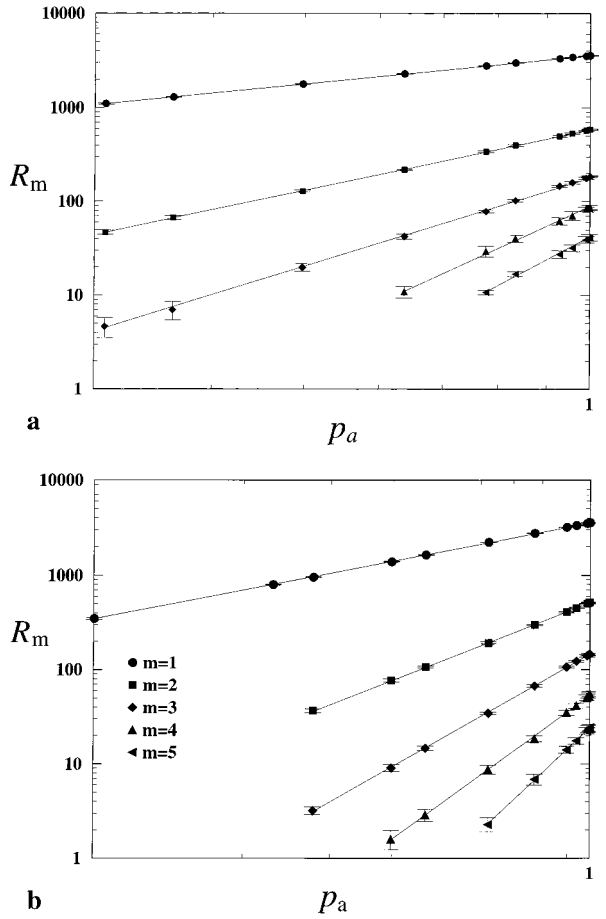

Figure 3. Plots of the number of cycles of m nodes within the system, R_m, against p_a, in logarithmic form, for the $\mathbf{AB}_2$ (a)[55] and for the $\mathbf{AB}_4$ polymerizations (b), with $m = 1, ..., 5$, showing how the data fit the power functions of eqs 3 and 4. The results of fitting these equations with noninteger and integer slopes are given in Table 1.

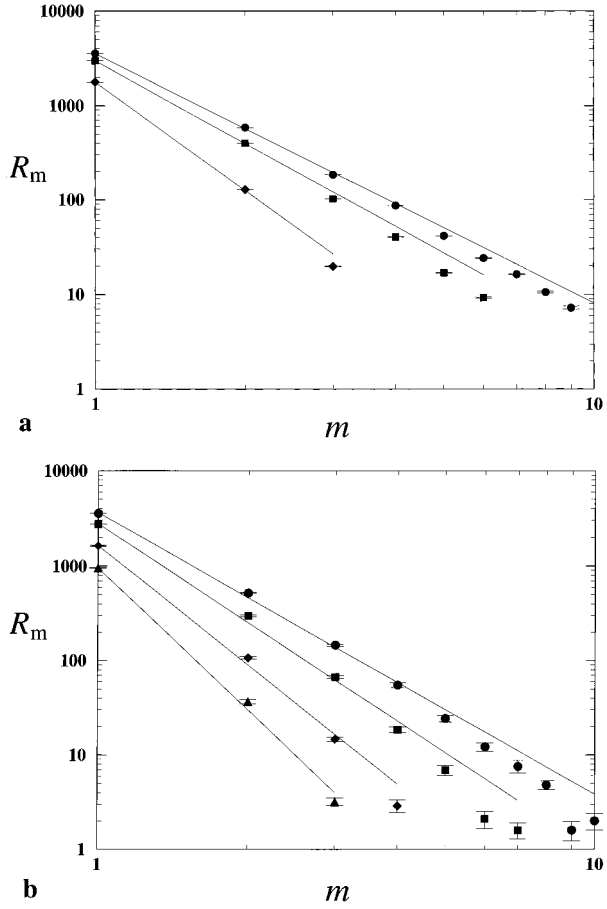

Figure 4. Plots in double logarithmic form of R_m at selected stages of the reaction, p_a, against m for (a**)** the $\mathbf{AB}_2$ system, $p_a = 0.498$ (diamonds), 0.834 (squares) and 1.000 (circles); and (b**)** for the $\mathbf{AB}_4$ system, $p_a = 0.276$ (triangles), 0.465 (diamonds), 0.772 (squares) and 1.000 (circles) As for the more extended $\mathbf{AB}_2$ system,[17] the final value of γ in part (a**)** is hardly different from *e***,** but in part (b**)** neither set of data quite fit a straight line.

is larger and the lattice representations are not so configurationally flexible, but for $m = 1$ and 5 the difference is a standard deviation, and forcing the integer on the analysis by using eq 4 causes little change

$$R_m = C_m p_a^{\,m} \tag{4}$$

to the C_m term. Thus, C_m and $C_{m'}$ are respectively 183.8-(±0.8) and 180.0(±1.9) when $m = 3$. Equations 3 and 4 were also found to be followed rather well by the $\mathbf{AB}_4$ system, and we record the corresponding values of $C_{m'}$, m' and C_m in Table 1; again the fitted values of m' are close to integers, and when the values of $C_{m'}$ and C_m are compared, little difference is seen.

We have noted previously that loop formation ($m = 1$) follows p_a throughout the polymerization of an $\mathbf{AB}_2$ system, the rationalization being that the chance, for an **A** group, of a neighboring **B** belonging to the same or to a neighboring molecule being constant throughout, for each type of **B** group, diminishes at the same rate:[17] apparently the local concentrations of the two types of group reflect fairly well the global values even toward the end of the simulation. For larger cycles, e.g., $m = 4$, the rings of that size form from hyperbranched structures that contain four nodes linked by three previous reactions. Such an arrangement may lie within a linear tetramer or—more likely—within a much larger branched molecule (where it might be found several times), so it is not immediately obvious that the simple power law might occur: here we see it is quite independent of f in these two molecules of very different branching potential (at least for $m < 6$). It presents in a simple manner the consequences of the competition between growth and cyclization within a large range of structural isomers as the system evolves. It is clear that as the reaction comes to a close, cyclization is enhanced relative to growth. If we knew how $C_{m'}$, m' and C_m depended upon m, we might obtain the total number of cycles in the systems, and so we now turn to that task.

For the present $\mathbf{A}-N(-\mathbf{B})_2$ system at selected values of p_a we have plotted R_m against m in a double logarithmic form,[13,14,17] as shown in Figure 4, where it may be seen that good straight lines are found for this kinetically obtained data. When fitted with the following function, appropriate to both kinetically produced and equilibrium-produced cycles (with $\gamma = 2.5$ in the latter case)[45,57]

$$R_m = A_p m^{-\gamma} \tag{5}$$

it transpired again,[11,14,17] as Figure 5 shows, that the two constants varied linearly with p_a, with $A_p = A_1 p_a$, ($A_1 = 3576.1(\pm 3.2)$), and γ falling linearly with p_a: $\gamma_p = 2.714(\pm 0.005) + (1 - p_a)2.543(\pm 0.050)$, so $\gamma_1 = 2.714$-(±0.005). (The subscripts to A and γ refer to the

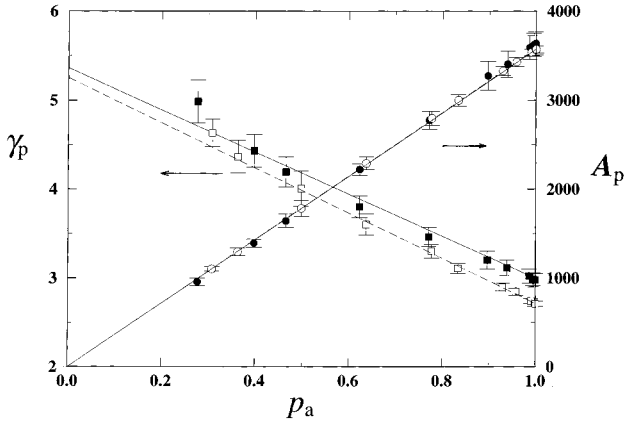

Figure 5. Plots of γ_p (squares) and A_p (circles) at selected stages of the reaction against, p_a (the latter plots pass through (0,0) and nearly coincide). Linear relationships have been found, at least for the $\mathbf{AB}_2$ system. The symbols are open for the $\mathbf{AB}_2$ system, and filled for the $\mathbf{AB}_4$ system.

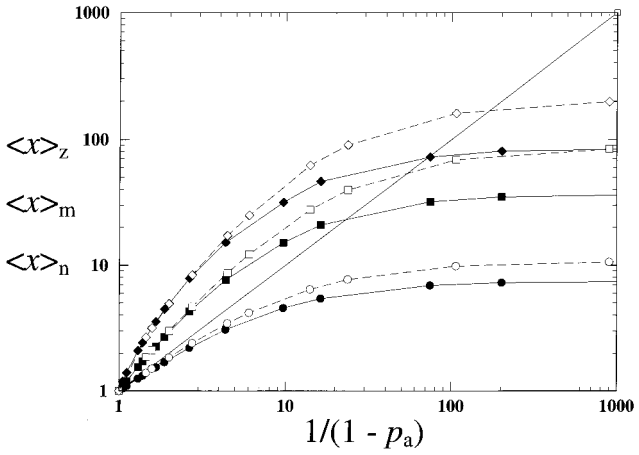

Figure 6. Plots of the number-average degree of polymerization, $\langle x \rangle_n$ (circles), the weight-average degree of polymerization, $\langle x \rangle_w$ (squares), and the *z*-average degree of polymerization, $\langle x \rangle_z$ (diamonds), against the Carothers function, showing how the Monte Carlo averages tend to limiting values as the polymerization progresses. The symbols are open for the $\mathbf{AB}_2$ system, and filled for the $\mathbf{AB}_4$ system. The diagonal line is the Carothers function, from which the Monte Carlo results diverge.

corresponding values of p_a.) For this $\mathbf{AB}_2$ representation the initial value of γ, γ_o, is 5.26, compared to 4.90 for the $\mathbf{A}-X-X-N-\mathbf{B}_2$ case, so loops are more favored over larger cycles with the present $\mathbf{AB_2}$ case throughout the course of the reaction. However, the final values of γ and γ_1, found for the two systems, are both interestingly indistinguishable from *e*. In terms of the ζ function,[57,58] $\zeta(x) = \sum m^{-x}$, for the present case the total number of cycles present at the end of the polymerization is predicted from eq 5 to be $A_1\zeta(2.714) = 1.227A_1$. Therefore, loops constitute 100/1.227 = 81.5% of the cycles.

By combining eqs 4 and 5, we find that a further simple relationship also holds when $f = 2$ for values of the two variables m and p_a

$$R_m = C_o\, {p_a}^m\, m^{-\gamma_1} \tag{6}$$

with $C_o = A_1$ or C_1′. In these respects the present $\mathbf{A}-N-\mathbf{B}_2$ monomer behaves like the other representation, $\mathbf{A}-X-X-N-\mathbf{B}_2$[17] though the leading terms differ, as the two monomers have a different ease of loop formation and different N_o values. This type of function has been found for cyclizations in linear step growths[57] and its behavior evaluated.[58]

It follows from the form of eq 6, as Figure 3 demonstrates, that larger rings form at considerably accelerating rates just as p_a approaches unity; but as the limiting behavior, $(dR_m/dp_a)_{p=1} = C_o m^{-(\gamma_1-1)}$, even then the smaller rings still form at more rapid numerical rates than do each of the large ones (so loops are 49% of the cycles that form just at the end). At the end of the polymerization the mean size of the cycles, $\langle m \rangle_{n,\infty}$, from eq 5 is given by

$$\langle m \rangle_{n,\infty} = \sum m R_m / \sum R_m = \zeta(\gamma_1 - 1)/\zeta(\gamma_1) \tag{7}$$

from which we find $\langle m \rangle_{n,\infty} = 2.027/1.227 = 1.65_2$ for this flexible monomer. The fraction of the nodes within cycles we obtain from $\langle m \rangle_{n,\infty}/\langle x \rangle_{n,\infty}$ as 0.1544 ($\langle x \rangle_{n,\infty}$ is obtained in section D below). By this method we find for the $\mathbf{A}-X-X-N-\mathbf{B}_2$ case $\langle m \rangle_{n,oo}/\langle x \rangle_{n,\infty}$ to be 0.114, whereas an inspection of the data array found only 0.101,[17] so the distribution function fitted over $m < 11$ predicts more large rings than are really present at higher values of m. In fact we cannot extend the form of eq 7 to obtain $\langle m \rangle_{w,\infty} = \sum m^2 R_m / \sum m R_m$, as $\sum m^{-0.714}$ is not bounded,[58-60] a further observation that suggests that eqs 5 and 6 cannot extend to very large values of m, where instead R_m must fall faster toward zero than eq 5 describes. (In contrast, during the reaction of $\mathbf{A}_2$ with $\mathbf{B}_3$ monomers, while the number of small cycles remains finite, the number of large cycles eventually explodes with m.)[49]

The more functional $\mathbf{A}-N-\mathbf{B}_4$ monomer behaves similarly, in that cycles do form and the smaller cycles predominate, but the larger cycles diminish in proportion much faster than the initial power law at each p_a value for which we show results, and the log−log plots of Figure 4b show that the trends are curved, even at the end of the polymerization. The final set of points on that plot ($p_a = 1.000$) have a γ for the first two which is 2.77_2, and over the first 17 points—where the curve steepens—the value rises to 2.97(±0.02), with $A_1 = 3552$-(±20)), so the power law is not really appropriate when $f = 4$ (The analysis gives much less weight to the later points not even shown on the figure when finding a straight line). However for comparison with the $\mathbf{AB}_2$ system, we may obtain from the data shown in Figure 4 the relationship that $\gamma_p = 2.97(\pm0.02) + (1 - p_a)2.40$-(±0.09), with just a little systematic drift, as shown in Figure 5. Similarly $A_p = 3582(\pm21)p_a$, though note that all the latter points are above the straight line. We presume that the extra scope for cyclizations in the monomer system is responsible for this more elaborate behavior (which occurs here within the range of m examined rather than being inferred, as before, as taking place at higher values of m, and is found in N_x too: see below). The value of A_p differs only a little from C_1 (3537(±9)), with which it is ideally identical, so the poorness of the fitting is not extreme for the leading term. We obtain with eq 7, adopting $\gamma_1 = 2.97$, $\langle m \rangle_{n,\infty} = 1.38_6$ and the fraction of nodes as cycles as 0.185. A significant fraction of the monomers is consumed in rings, but the fraction is just 20% greater when $f = 4$ than when $f = 2$.

(D) Molecular Weight Development. We plot in Figure 6 $\langle x \rangle_n$, $\langle x \rangle_w$, and $\langle x \rangle_z$ against the Carothers function, $1/(1 - p_a)$. It may be seen that each of these rises in the same way, independent of *f*, to begin with,

Table 2. Degrees of Polymerization and Polydispersities at the End of the Simulations

$\mathbf{A}-N-\mathbf{B}_f$	t_e[a]	$\langle x\rangle_n$	$\langle x\rangle_w$	$\langle x\rangle_z$	$\langle x\rangle_w/\langle x\rangle_n$	$\langle x\rangle_z/\langle x\rangle_w$
$f = 2$	5M	10.72(±0.07)	86(±2)	204(±13)	8.0(±0.2)	2.7(±0.2)
$f = 4$	2M	7.48(±0.04)	37.1(±0.2)	85.8(±0.4)	4.96(±0.04)	2.31(±0.02)
$f = 2$[b]	5M	14.47(±0.25)	166(±10)	485(±50)	11.5(±0.7)	2.9(±0.3)

[a] CHOICE cycles—or time units—used at end of simulation on the 60^3 lattice. Initial conditions noted in the footnotes of Table 1. [b] With the six-site $\mathbf{A}-X-X-N(-\mathbf{B})_2$ lattice representation.[17]

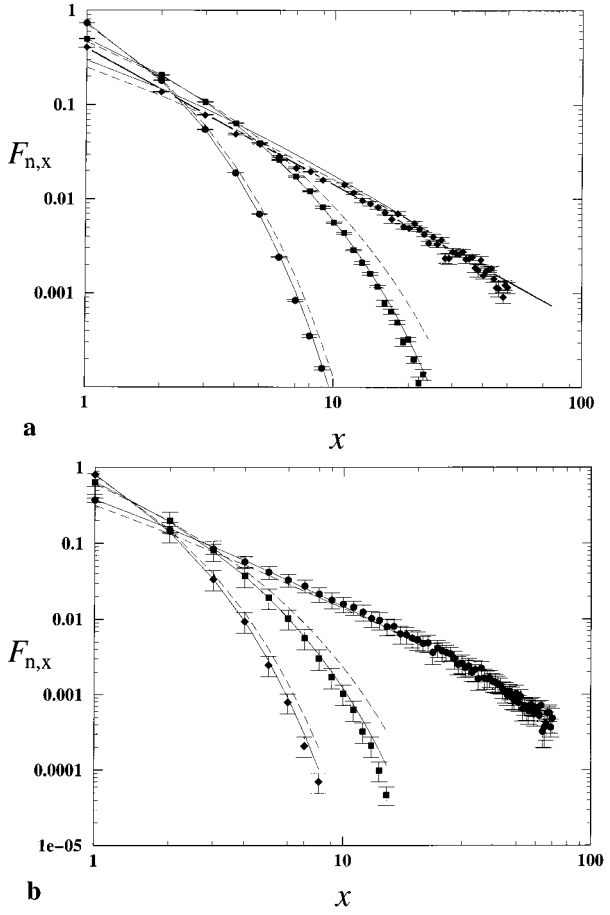

Figure 7. Number fractions of molecules of different sizes plotted against x for (a**)** the $\mathbf{AB}_2$ system, and (b**)** for the $\mathbf{AB}_4$ system at the following values of p_a: (a**)** $p_a = 0.308$ (circles), 0.637 (squares), and 1.000 (diamonds), **(**b**)** $p_a = 0.230$ (circles), 0.772 (squares), and 1.000 (diamonds). In each case a pair of curves is shown, the upper being the simple Flory expression of eqs 9 and 10, and the lower, more fitting curve being that obtained with p_e replacing p_a in those equations (p_e counts only the bonds that created the trees). Each final set of data show strong deviations from the Flory expression, and are better fitted—at least initialy—by a straight line, eq 11.

but the initial linearity of the variables with $1/(1 - p_a)$ then fails, and they all turn toward limiting values (as do the polydispersities), the final measures of molecular weight being lower for the $f = 4$ case than for the $f = 2$ case: we report the values obtained at the end of the simulation in Table 2. Doubling f has reduced the mean molecular weights when all the **A** groups have been consumed by roughly a factor of 2; the factor is just 1.43 for $\langle x\rangle_n$, but larger at 2.32 for $\langle x\rangle_w$, and a little higher (2.38) for $\langle x\rangle_z$, so the final polydispersities are also reduced. If cyclizations are not absolutely prevented polydispersities and molecular weights are finite. When we plotted the number fraction of molecules containing cycles, $F_{n,c}$, against $\langle x\rangle_n$ in Figure 2, it was seen that the linear limiting behavior allows us to extrapolate to find the values of $\langle x\rangle_{n,\infty}$: 10.72(±0.07) for $f = 2$ and 7.50(±0.04) for $f = 4$. We recall that with the $\mathbf{A}-X-X-N(-\mathbf{B})_2$ representation the value of $\langle x\rangle_{n,\infty}$ was 14.3,[17] so distancing the **A** group from the **B** groups by including two X spacers within the monomer enhanced growth over cyclization by a further 34% in terms of $\langle x\rangle_n$. The entries in Table 2 record that as the **A** and the **B** groups within the monomer are brought closer together and the latter increased in number, the final degrees of polymerization and their polydispersities are all reduced by the greater ease with which cyclization occurs. A simple measure at the end of the reaction of the relative proportion of growth and cyclization is provided by the ratio $(\langle x\rangle_{n,\infty} - 1)$:1,[17] for at the end of the polymerization each molecule contains a cycle, from which one or more branches extend, and as we have already noted, the slopes on the nearly linear curves of Figure 2 indicate this proportion during the course of the polymerizations. If, in estimating the extent of reaction we included only those bonds that accompanied growth, then we obtained a factor, $p_e < p_a$, which exactly provided $\langle x\rangle_n$ as $1/(1 - p_e)$ throughout the polymerization.

(E) Molecular Weight Distributions. We have obtained the number and weight distributions of the products from the records and compare these with values obtained using the theoretical equations given by Flory for $\mathbf{AB}_f$ monomers[1] (N.B. our f is one less than his). We examine the Monte Carlo results displayed in Figures 7 and 8 against this standard. Qualitatively both quantities do decrease smoothly with x, as Flory predicts.[1] Cycle formation was omitted from his treatment, each molecule retaining to the end one **A** functional group. He introduced a branching probability factor, $\alpha = p_b = p_a/f$, and a term β

$$\beta = \alpha(1 - \alpha)^{f-1} = p_a(1 - p_a/f)^{f-1}/f \qquad (8)$$

The number of molecules of size x was given by

$$N_x = N_o[(1 - \alpha)/\alpha]\omega_x\beta^x$$
$$= N_o(f - p_a)p_a^{-1}\omega_x\beta^x \qquad (9)$$

and the weight of molecules of size x was given by $W_x = xN_x/(\sum xN_x)$ and thus was

$$W_x = [(1 - \alpha)/\alpha][1 - \alpha f]x\omega_x\beta^x$$
$$= [(f - p_a)/p_a][1 - p_a]x\omega_x\beta^x \qquad (10)$$

where

$$\omega_x = (fx)!/((fx - x + 1)!x!)$$

is the number of isomers that may form from $x\mathbf{AB}_f$ monomers[1,23] (in the absence of any sterric effects). We have plotted the data in the normalized forms of $F_{n,x} = N_x/N_o$ and $F_{w,x} = xN_x/N_o$. The distributions were also calculated by replacing p_a with values of p_e, within

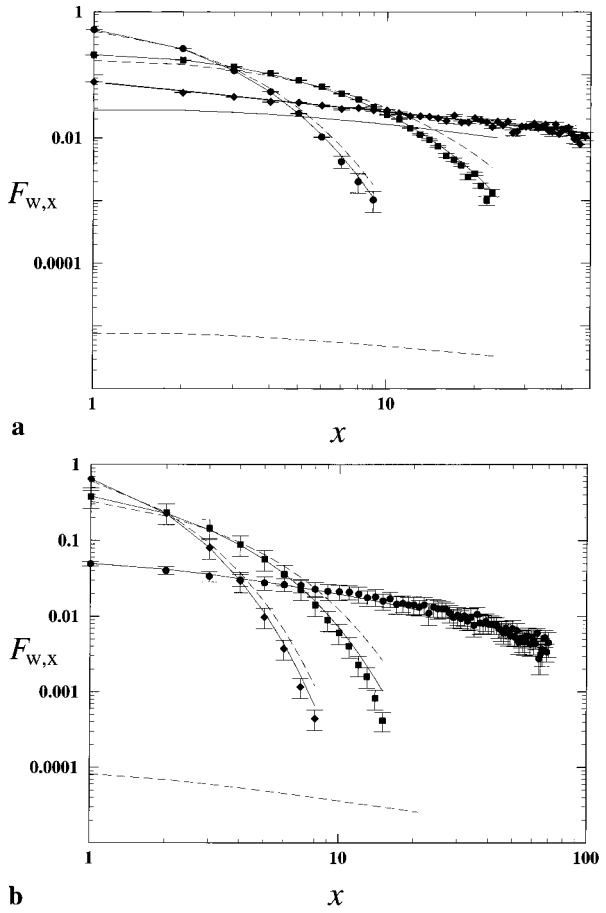

Figure 8. Weight fractions of molecules of different sizes plotted against x at the following values of p_a: (a) for the $\mathbf{AB}_2$ system, $p_a = 0.308$ (circles), 0.637 (squares), and 1.000 (diamonds); (b) for the $\mathbf{AB}_4$ system, $p_a = 0.230$ (circles), 0.772 (squares), and 1.000 (diamonds). In each case a pair of curves is shown, the dashed line being the simple Flory expression of eq 10, and the full, more fitting curve being that obtained with p_e replacing p_a in those expressions. For the data at the end both curves strongly deviate, and are better fitted by a straight line, eq 13.

which were included only bonds linking the residues into a branched framework or tree,[17] and which gives the model's value of $\langle x\rangle_n$ at all times when used in the Carothers function, as we noted above. By omitting the cyclizations from p_a, we crudely allow for the previous neglect of cyclization.

For the $\mathbf{A}-N-\mathbf{B}_2$ system the Flory distributions for number and weight of the oligomers is in quite good agreement with the model's results when p_a is small, and the deviations that are found at larger values of p_a may be reduced if the intermolecular reactions only of the **A** groups are included in p_a, but they remain systematically greater than the standard deviation (Figure 7). At the end of the reaction, when the points are seen to lie on a straight line rather than a curve in the double logarithmic plot, the modification is unable to save the Flory approach, and the following power law is found to apply for $0 < x < 48$:

$$N_x = N_{1,\infty}\, x^{-\chi_n} \tag{11}$$

In this $\mathbf{A}-N-\mathbf{B}_2$ case $\chi_n = 1.488(\pm 0.021)$ and $N_{1,\infty} = 1841(\pm 6)$. χ_n is indistinguishable from 1.50, and cyclization has transformed the functions[1] appropriate to Cayley trees into this form for graphs grown in three dimensions. The form of eq 11 is apparently independent of the monomer representation, for we found $\chi_n = 1.5$ in the study of the $\mathbf{A}-X-X-N(-\mathbf{B})_2$ model too, though the values of $N_{1,\infty}$ differ. (For quite different reasons others[11] have found an initial $x^{-1.5}$ dependence for N_x from an examination of self-condensing vinyl polymerization, but they omitted cyclizations.) Since each molecule finally contains a cycle, the final number can be obtained by summing either eq 4 or eq 11. When $p_a = 1.000$, the initial number of molecules, the number-average degree of polymerization at the end of the polymerization, the final number of molecules present, the final number of cycles present, and the constants in the two equations, are related by means of zeta functions:[17,58−60]

$$N_o/\langle x\rangle_{n,\infty} = N_\infty = N_{1,\infty}\sum x^{-\chi_n} = N_{1,\infty}\zeta(1.488) = 2.661N_{1,\infty}$$

$$= \sum R_m = C_o\sum m^{-\gamma_1} = C_o\zeta(2.714) = 1.227C_o \tag{12}$$

This clearly relates both $N_{1,\infty}$ and C_o (or A_o) inversely to $\langle x\rangle_{n,\infty}$. (In an experimental study, p_e might be estimated from p_a at any stage of the reaction and $\langle x\rangle_{n,\infty}$, as the latter is sufficient to obtain C_o.)[17,58]

At the end of the $\mathbf{A}-N-\mathbf{B}_2$ polymerization the weight distribution is also better given by a power law

$$W_x = N_{1,\infty}\, x^{-\chi_w} \tag{13}$$

(here $W_x = xN_x$) though at lower values of p_a the Flory function of eq 10 or its modified form (replacing p_a with p_e) are fairly good. The reason the final unmodified curve appears on the Figure 8 at all is that p_a is only 0.999 974. The data provide $\chi_w = 0.488(\pm 0.021)$, any discrepancy from 0.500 perhaps reflecting the fact that the p_a was not quite 1.000 000.

We have realized before[17] that a weight distribution function cannot follow $W_x = N_{1,\infty}\, x^{-0.50}$ much beyond the fitted range of x, for the total weight in the system, given by $N_{1,\infty}\sum x^{-0.50}$, would not be N_o but rather would be infinity if x proceeds to infinity, as the series is not bounded when the exponent is greater than -1.00.[58−60] From this behavior of the distribution functions our present model thus also predicts a finite size to the graphs produced (as noted in the previous section of mean sizes), and W_x (and N_x too) must fall to zero at some point above $x = 48$. This conclusion is independent of the size of the Monte Carlo sample, and is presumably because of the accumulating chance within large fractals that a cyclization will prevent an **A** group reacting externally with a **B** group: this may reflect a real excluded volume effect around the **A** groups experienced by the neighboring and potentially reacting molecules that promotes the return of the random branching walk by an intramolecular reaction well before x can rise to infinity. (The congestion is a feature of the lattice models, and is never so severe as in a dendrimer, whose smooth growth away from the root of the tree creates at each generation f^k new attached residues, but the space for them rises only with k^3.)

With the $\mathbf{A}-N-\mathbf{B}_4$ system the same pattern of behavior is demonstrated in Figures 7 and 8, and even near the beginning of the reaction, when $p_a = 0.28$, the omission of cyclization steps from the extent of reaction used in calculating the number and weight fractions

produces much better curves. The final set of points is much better fitted by this procedure, for the Flory line lies at the bottom of the weight fraction graph. At the end of the simulation the first 10 points apparently fit well to a power law, as in eq 11, with $\chi_n = 1.3616(\pm 0.0095)$ and $N_{1,\infty} = 4337(\pm 48)$, and over the first 20 points the values obtained are higher, as the curvature matters, and we found $\chi_n = 1.399(\pm 0.011)$ and $N_{1,\infty} = 4415(\pm 79)$. Since for the first two species $\chi_n = 1.29_0$, it appears that this final set of points lies on a curve and that the initial slope is significantly less than 1.50, two characteristics differing from the $\mathbf{AB}_2$ systems. It is evident that the slope becomes steeper as x rises beyond about 12. The arguments about W_x falling off at large x seem to be justified in this case within the second part of the range explored by the Monte Carlo model. The curvature in these log−log plots probably joins the curvature noticed in the similar R_m against p_a plots of Figure 4b in reflecting the greater tendency in the present system ($f = 4$) for cycles to form.

The self-returning random walks formed in this branching step growth are of a finite size, as are the pendant branches: we have seen how the Carothers equation, with p_e as argument, gives $\langle x \rangle_n$, but that the Flory distribution functions cannot be saved by that expedient. Now we turn to an examination of the tree and graph structures that develop.

(F) Recognizing the Oligomer Structural Isomers through Node Priority Values [ ].[17] An analysis procedure[49] ordered the nodes within each molecule by an integer i, based upon their extent of reaction (0, 1, 2, ..., $f + 1$) and then according to the sum of the extents of reaction of the neighbors (1, 2, 3, ..., $(f + 1)^2$) and so on. For the $\mathbf{AB}_2$ system the method[17] generally placed first the node that bears a loop and then turned to centrally located branch sites. We term these numbers node priority values, and have used only two sets here. As some structures in the $\mathbf{AB}_2$ system might have a node with a higher second priority than the loop, we included an overriding rule that such a node always had $i = 1$, but in the $\mathbf{AB}_4$ system, the possibility that another node might have reacted more than three times might displace the loop node to the second or an even lower position (and such an overriding rule was not used). The loop node is generally equivalent to the root node of a tree (though the presence of the loop converts the tree into a graph).[60,61] Had we adopted a rule that the **A** group was at the *root* of the tree, it would have conflicted with giving priority to the extent of reaction: it would have provided an exclusively fractal account of the polymerization, and so would have not held to the end, when no **A** groups remained. In Schemes 1 and 2 there are a number of examples of molecules with their nodes ordered to illustrate the method, and in Scheme 1 the numbers in braces, [ ], are the priority values in two groups of x. The molecule is quite readily identified from the priority values that the analysis routine returns. Note that the locations of any unreacted **A** groups are not indicated, so the number of trees/branched isomers differs from that provided by ω_x above, and that which an NMR analysis might provide.

(G) The Composition of the Products, the Distribution of Extent of Reaction over their Nodes, and a Kirchhoff Representation of their Structures. The branch structure of each product of size x was obtained from the model's data records of the developing pattern of bonding between the nodes, at intervals during each reaction, after a procedure had arranged the information in a suitable form. At a global p_a the individual isomers of each particular degree of polymerization, x, were identified and their proportion found, measures obtained of the mean extent of reaction of the nodes or residues at each position in the assigned order within the mean vector $\langle \mathbf{P}_{x,p} \rangle$, and the mean framework of such the tree and graph isomers was obtained in a mean adjacency[61] or Kirchhoff matrix, $\langle \mathbf{K}_{x,p} \rangle$. No previous method provides such information.

$\langle \mathbf{P}_{x,p}[i] \rangle$ contains in the elements 1, ..., i, ..., x the mean number of reactions suffered by the functional groups on each of the i-ordered nodes of all molecules of a size, x, at a global p_a. For a particular isomer the $\mathbf{P}[i]$ values correspond to the first set of node priority values. For the monomer the entries are either 0 or 2, as only it may contain a residue that has not reacted at all, and unless it reacts with itself, it does not remain a monomer. For the other oligomers the values have two different patterns, depending on whether they are linear and branched, or cyclic. The values for the linear $\mathbf{AB}_2$ molecules have the following structures [2, 2, ..., 2, 1, 1], the branched ones containing one or more "3" nodes, and for each of these an extra "1" node: [3, 2, ..., 2, 1, 1, 1], [3, 3, ..., 1, 1, 1, 1], and so on. The cyclic molecules have a different pattern: [2, 2, ..., 2, 2, ..., 2, 2], [3, 2, ..., 2, 2, ..., 2, 1], [3, 3, ..., 2, 2, ..., 1, 1], and so on, the number of branch points rising until—if x is even—every element is either 3 or 1. If x is odd, the modal ordered node of the graphs must have reacted two times. The entries in the second series are always symmetrical about the mean for odd and even values of x, but the

Scheme 1. Monomer, Dimer, Trimer, and Tetramer Structures for the $\mathbf{AB}_2$ and $\mathbf{AB}_4$ Systems, Their Characterizing Priority Values [ ], and Some Kirchhoff Matrices and P Vectors[a]

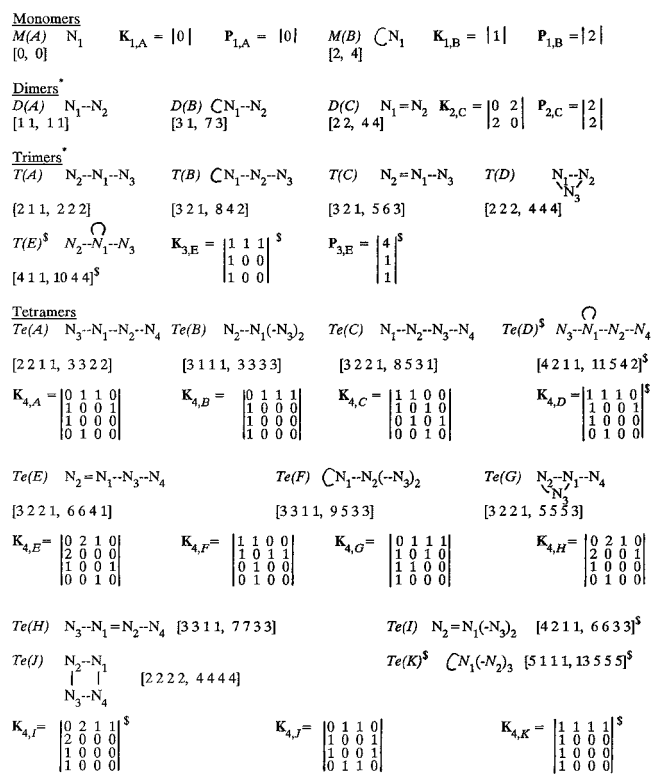

[a] Scheme footnotes are as follows: (*) **K** matrices and **P** vectors of all the $\mathbf{AB}_2$ forms have been given before[17] (note that **A** groups are not identified on the acrylic structures); ($) peculiar to the $\mathbf{AB}_4$ system.

Scheme 2. Hexamer Molecules Predominating at the Halfway Stage (Node Numbers Following Priority Values)[a]

p_a = **0.498 (with N for f = 2) and** *0.465* **(with N** *and N* **for f = 4),** [p_a = 0.500], from the **A**--*X*--*X*--*N*(-**B**)$_2$ study[17].

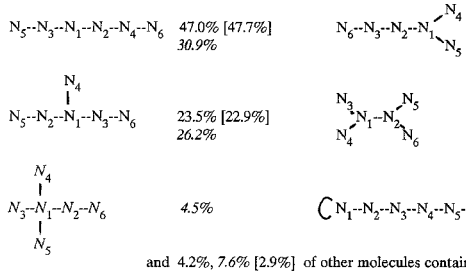

and 4.2%, *7.6%* [2.9%] of other molecules containing loops and rings.

Hexamer molecules predominating towards the end of reaction:
p_a = **0.929 (with N for f = 2) and** *0.897* **(with N** *and N* **for f = 4),** [p_a = 0.890], from the **A**--*X*--*X*--*N*(-**B**)$_2$ study[17].

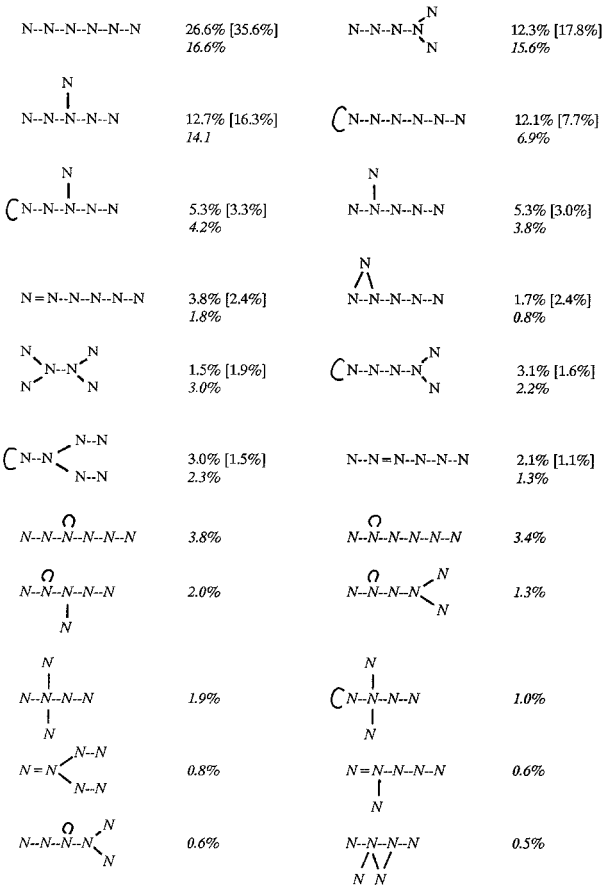

Hexamer molecules predominating at the end of reaction (node numbers follow priority values):
p_a = **1.000 (with N for f = 2) and** *1.000* **(with N** *and N* **for f = 4),** [p_a = 0.999], from the **A**--*X*--*X*--*N*(-**B**)$_2$ study[17].

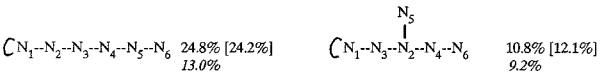

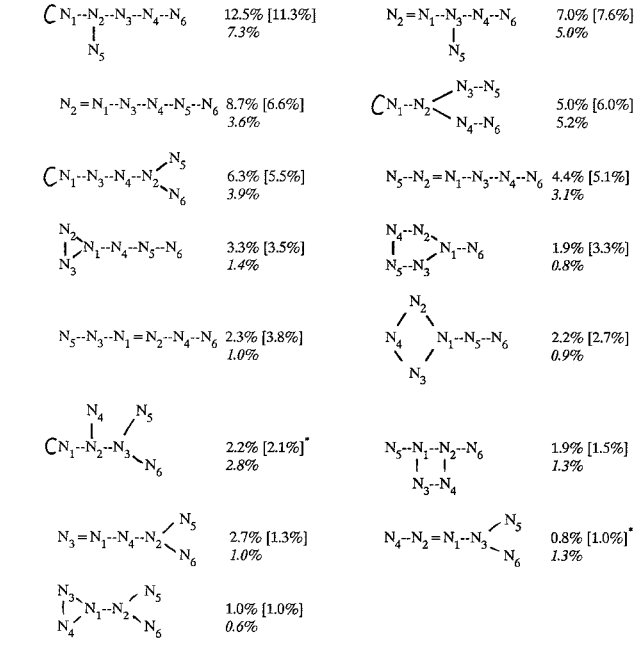

Hexamers peculiar to the AB_4 system:

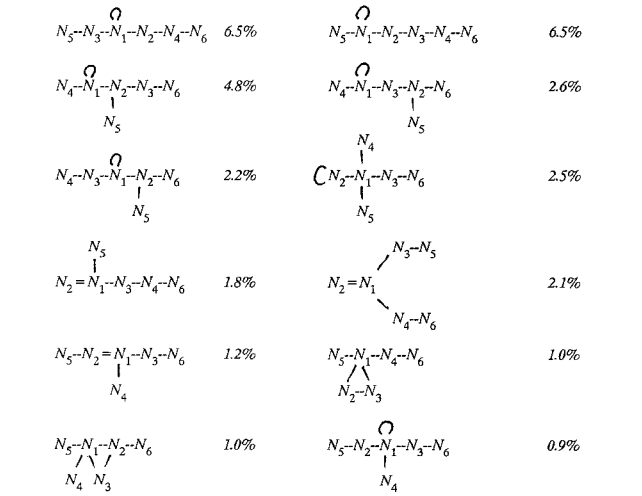

Some hexamers from below the 1% level:

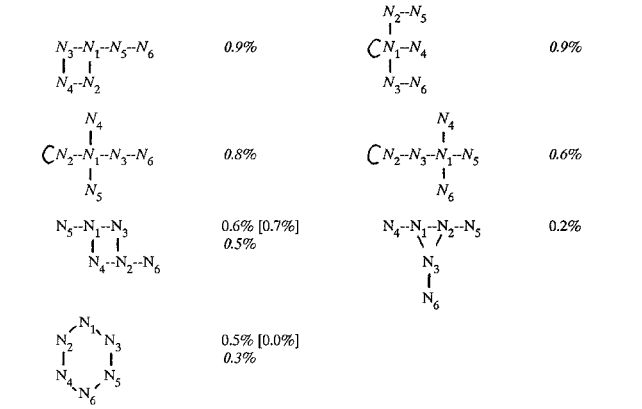

[a] Scheme footnote is as follows. (∗) These are not distinguishable with two sets of priority values; their proportions for that "oligomer" were found from ⟨**K**$_{6,1}$[**1,1**]⟩,[17] as only one isomer has a loop. No such ambiguities deriving from the node priority values occur at the pentamer stage.

proportion of branch and end units to extenders depends on the populations produced by the random process and remains to be established. A number of different structures may have the same first priority values, as wehave

listed for the hexamers,[17] but they may generally be distinguished with the second set, at least when x is small (see footnote *a* in Scheme 2). The pattern of first node priority values for the $f = 4$ oligomers is more varied around the general pattern [5, ..., 4, ..., 3, ..., 2, ..., 1], as may be seen in the examples of Scheme 1, for the x integers may be grouped in many different ways, yet have the same sum, $2x$. It is possible to construct the framework for the oligomer from these values, for example, tetramers *C*, *E*, and *G* have the same set of first priority values, but may be distinguished by the second set. The more cumbersome Kirchhoff matrix is, of course, definitive, but was thought to be less convenient for data analysis.

Within $\langle \mathbf{K}_{x,p}[i,j] \rangle$, the element on the ith row and in the jth column indicates the frequency with which the ith and jth nodes of an $x$mer are chemically linked to each other through an **A**−**B** bond at a global p_a. This provides the mean structural information for isomers of the trees and the graphs taken together. The value of the [1,1] element measures the incidence of a loop at the node with the highest extent of reaction, a loop having been formed by the linking of **A** and **B** groups attached to the same node; for the $\mathbf{AB}_4$ system, a loop may also be found at the node with the second, third or other priority (if other nodes have reacted more than three times). In these system the chemistry of the monomer determines that only one node of a molecule can bear a loop, and the other diagonal entries for that molecule are zeros. The sum of the elements of the ith row or column of the $\langle \mathbf{K} \rangle$ matrix is $\langle \mathbf{P}[i] \rangle$, the $\langle \mathbf{K}[1,1] \rangle$ and any other $\langle \mathbf{K}[i,i] \rangle$ entry being doubled for the summation, as two groups are consumed by the formation of a loop. The mean value for $\langle \mathbf{P}_{x,1}[i] \rangle$ taken over all the i is 2.000 when each **A** group has reacted with one **B** group, throughout the polymerization the fraction of cycles within molecules of size x is given by $(\sum \mathbf{P}_{x,p}[i] - 2(x - 1))/2$,[17] and the excess of $\langle \mathbf{P}_{x,p}[x] \rangle$ over 1.000 measures the fraction of cycles of size $m = x$.

A single branching parameter has been used by some, but they also have observed that "it is doubtful if only one parameter would be able to give a good characterization of a broadly distributed hyperbranched polymer".[5] $\langle \mathbf{P} \rangle$ and $\langle \mathbf{K} \rangle$, each with several elements to describe the linkages, are an advance and by our method are obtained at any time for each value of x. Some scheme of ordering the nodes is required for this purpose (and for the trees, a scheme might be based on the distance from the **A** groups). The complement to $f + 1$ of the $\langle \mathbf{P}[i] \rangle$ elements measures the scope for a later reaction, either during the polymerization itself, as shown in Figure 9, perhaps if a second batch of monomer were to be added, or, if $p_a = 1$, then for a reaction with $\mathbf{A}_2$ dimers or $\mathbf{A}_x$ hyperbranches to create, e.g., a network, as when a paint sets. In the latter context, of course, loops are a waste of chemistry.

The structural isomers of oligomers are shown in Schemes 1 and 2, where their node priority values are also given. The **K** matrixes and **P** vectors are also given for the new trimer and tetramers in Scheme 1. The proportions of these oligomers at three stages of the reaction are given in Tables 3 and 4. The mean Kirchhoff matrices we obtained for these and some representative higher oligomers are also given in Scheme 3. When x is small the values of the elements are directly related to the proportions of the related oligomers,[17] but for the higher oligomers, the matrix elements are fewer than the number of possible isomers, and a mean representation is provided of the many structures present. The richness of the information available from the model is illustrated by Scheme 2, where the predominant structural hexamers are indicated at three stages of the polymerization. It is clear that there is a considerable evolution in the structures of molecules of even the one size as the reaction proceeds. This is particularly so when $f = 4$.

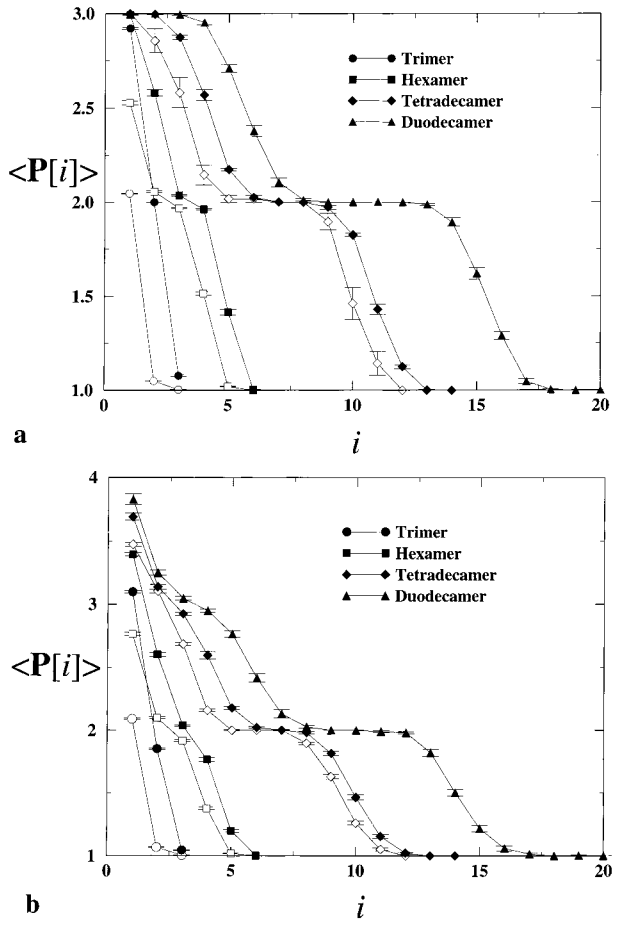

Figure 9. Plots of $\langle \mathbf{P}[i] \rangle$ against the node number i for the trimers (circles), the hexamers (squares), and the tetradecamers (diamonds) halfway through the polymerization (open symbols) and at the end (filled symbols); the duodecamers (triangles) are shown at the end of the polymerization only, for only a few simulations obtained such molecules at the halfway stage. Observe that the final plots are centro-symmetric for the $\mathbf{AB}_2$ system in (a), but not so for the $\mathbf{AB}_4$ system in (b), for which some of the nodes have reacted four or even five times, so at low values of i some $\langle \mathbf{P}[i] \rangle$ are greater than 3.000.

When the entries in Table 3 are considered, it is apparent that the proportion of looped monomer *B* is almost the same in the two systems at the halfway stage, but when p_a is about 0.9, the looped form is almost twice as frequent in the $\mathbf{AB}_4$ form, and is complete in both at the end. At the halfway stage the predominant dimers and trimers are the linear *A* isomers, but there is an almost double proportion of cyclized forms in the $\mathbf{AB}_4$ case. At the end the proportion of the looped form *B* is a little higher for $f = 4$ than for $f = 2$. As two looped trimers may be found for the $\mathbf{AB}_4$ case (*B* and *E*), the loop is more frequent than in the trimers formed from the $\mathbf{AB}_2$ monomer; in the dimers the looped form is also more frequent: loop formation there is favored over the ringed dimer.

Table 3. AB_f Monomer, Dimer, and Trimer Compositions at Three Stages during the Reaction[a]

		monomer		dimer			trimer				
f	p_a	X_A	X_B	X_A	X_B	X_C	X_A	X_B	X_C	X_D	X_E[b]
2	0.498	0.912	0.088	0.943	0.043	0.014	0.949	0.035	0.012	0.004	
4	0.465	0.904	0.096	0.911	0.074	0.015	0.919	0.049	0.016	0.004	0.012
2	0.929	0.649	0.351	0.464	0.401	0.135	0.503	0.346	0.111	0.039	
4	0.897	0.444	0.556	0.476	0.428	0.096	0.481	0.313	0.097	0.024	0.080
2	1.000	0.000	1.000	0.000	0.747	0.253	0.000	0.701	0.221	0.078	
4	1.000	0.001	0.999[c]	0.002[c]	0.808	0.190	0.003[c]	0.612	0.193	0.045	0.147

[a] The X values are number fractions of the structures shown in Scheme 1. [b] This isomer forms from only the $\mathbf{AB}_4$ monomer. [c] The value of p_a was only 0.999 74.

Table 4. AB_f Tetramer Compositions at Three Stages during the Reaction[a]

f	p_a	X_A	X_B	X_C	X_D[b]	X_E	X_F	X_G	X_H	X_I[b]	X_J
2	0.498	0.816	0.137	0.027	–	0.008	0.006				
4	0.465	0.742	0.179	0.030	0.016	0.010	0.011				
2	0.929	0.448	0.074	0.250	–	0.086	0.066	0.044	0.019	–	0.014
4	0.897	0.402	0.096	0.187	0.098	0.062	0.072	0.033	0.023	0.014	
2	1.000	0.000	0.000	0.513	–	0.185	0.134	0.089	0.043	–	0.035
4	1.000	0.000	0.000	0.384	0.199	0.116	0.137	0.066	0.046	0.027	0.015

[a] The X values are number fractions of the structures shown in Scheme 1. [b] Formed from only the $\mathbf{AB}_4$ monomer.

We now consider the tetramer compositions, the structural isomers being shown in Scheme 1 and the proportions being given at three stages of the reaction in Table 4. Halfway through the reaction both monomers provide mainly the linear form, *A*, the branched form *B* being the next most frequent, such uncyclized forms being as much as 95.3% for $\mathbf{AB}_2$ and still 92.1% for the $\mathbf{AB}_4$ form with more scope for branching. The looped tetramer *F* is slightly more favored for the $\mathbf{AB}_2$ system, and the two-node form *E* being favored for the $\mathbf{AB}_4$ system at the start and, it transpires, at each subsequent stage. The looped tetramer *D* can only form from the latter monomer: it is present at the halfway stage to a small extent, and accumulates until it reaches a 20% proportion at the end. The other isomer possible only in the $\mathbf{AB}_4$ system, *I*, has two nodes in the ring, and is found much less frequently even at the end. Four-node cycles, *J*, are more frequent with the $\mathbf{AB}_2$ system than the other, which has more **B** functional groups at shorter distances ($^7/_3$) from the root **A** group in the linear precursor. In each system the individual linear and branched forms diminish in proportion as the reaction continues, and vanish during the final stages in keeping with eq 2 and Figure 2 for the system as a whole. The number of forms present at the >1% level is just six for the $\mathbf{AB}_2$ system, with the linear looped form *C* predominating, but it is only about 38% of the structures in the $\mathbf{AB}_4$ mixture, where there are eight at the >1% level. The molecule *K*, with five groups consumed on the looped node, is just below that threshold, at about 0.9%.

The single elements of the $\langle\mathbf{K}\rangle$ matrices and $\langle\mathbf{P}\rangle$ vectors of the monomers (Scheme 3) directly measure the proportion in which a loop has formed, any other reaction taking the molecule out of that class. For the dimers, $\langle\mathbf{K}[1,1]\rangle$ measures the fraction with a loop, and the part of $\langle\mathbf{K}[2,1]\rangle$ and $\langle\mathbf{P}[2]\rangle$ greater than 1.000 measures the fraction of molecules in a two-residue cycle. The $\langle\mathbf{K}\rangle$ matrices and $\langle\mathbf{P}\rangle$ vectors themselves indicate initially that the trimers and tetramers are mainly linear, for the inner elements are about 2.0. When p_a is about 0.9 one node, N_1, has reacted 2.5 times, so about half the molecules contain a branch, and at the end that process is complete: if $\langle\mathbf{P}_{x,1}[1]\rangle$ is less than 3.000, it is because there is a proportion of molecules that have all the residues in a cycle, as $\langle\mathbf{P}_{x,1}[x]\rangle$ also measures. Among the tetramers the role of N_3 changes from being pendant to N_1 to being a link between N_1 and N_4.

In Scheme 2 we have tabulated, as examples of the moderately sized molecules, the predominant hexamer structures present at three stages of the reaction, when p_a is about 0.5, 0.9, and 1.0. Even a quick glance discovers significant changes as the reaction progresses. The results for the $\mathbf{AB}_2$ system are given in normal type, underneath them are the compositions for the $\mathbf{AB}_4$ system in *italics*, and in brackets [ ] are given the values from the study of the $\mathbf{A}-X-X-N(-\mathbf{B})_2$ system.[17] When p_a is about 0.5 the proportion of the four uncyclized isomers is about the same for the two $\mathbf{AB}_2$ systems, though the $\mathbf{A}-N(-\mathbf{B})_2$ has a (50%) greater tendency to cyclize, as measured by the proportion of molecules containing loops and rings. This tendency is nearly twice as much again for the $\mathbf{A}-N(-\mathbf{B})_4$ system. The linear molecule is less prominent and the branched structures more prominent when $f = 4$, the structure with the four branches on one node being about 4.5%.

When p_a is about 0.9, there are distinct differences in the population proportions for the two $\mathbf{AB}_2$ systems. The linear form derived from the present $\mathbf{A}-N(-\mathbf{B})_2$ momomer is less frequent (down from 36% to 27%), and other comparisons show that the proportion of looped and ringed structures is correspondingly higher. This may reflect a little the different points on the p_a range we have used, but it also probably reflects the greater ease of cyclization of the $\mathbf{A}-N(-\mathbf{B})_2$ system: the manner in which the monomer is mapped onto the lattice influences the isomer populations. The effect of bringing the **A** and **B** groups closer together is enhanced by increasing their number, as may be seen by inspecting the oligomers formed by the $\mathbf{A}-N(-\mathbf{B})_4$ system: the linear form is substantially lower in proportion, but the apparent scarceness of the linear looped form is compensated by three forms containing a loop where it is born by a node near the center of the molecule (these forms are shown at the end of that section).

At the end of the reaction, the proportions of the sixteen main species are the same to within 1% for both $\mathbf{AB}_2$ systems (except for two molecules with $m = 2$), suggesting strongly that under the conditions of the simulation—only a trace of "solvent" present—the two

Scheme 3. Mean Kirchhoff Matrices and P Vectors for AB_2 and AB_4 Oligomers at Selected Stages of the Reaction[a]

Monomers

AB_2

$\mathbf{K}_{1,0.5} = |0.088|$ $\mathbf{P}_{1,0.5} = |0.175|$ $\mathbf{K}_{1,0.9} = |0.649|$ $\mathbf{P}_{1,0.9} = |1.298|$ $\mathbf{K}_{1,1} = |1.000|$ $\mathbf{P}_{1,1} = |2.000|$

AB_4

$\mathbf{K}_{1,0.5} = |0.096|$ $\mathbf{P}_{1,0.5} = |0.192|$ $\mathbf{K}_{1,0.9} = |0.556|$ $\mathbf{P}_{1,0.9} = |1.113|$ $\mathbf{K}_{1,1} = |0.999|$ $\mathbf{P}_{1,1} = |1.997|$

Dimers

AB_2

$\mathbf{K}_{2,0.5}$ =

0.043	1.014
1.014	0.000

$\mathbf{P}_{2,0.5}$ =

1.099
1.014

$\mathbf{K}_{2,0.9}$ =

0.401	1.135
1.135	0.000

$\mathbf{P}_{2,0.9}$ =

1.937
1.135

$\mathbf{K}_{2,1}$ =

0.747	1.252
1.252	0.000

$\mathbf{P}_{2,1}$ =

2.747
1.253

AB_4

$\mathbf{K}_{2,0.5}$ =

0.074	1.015
1.015	0.000

$\mathbf{P}_{2,0.5}$ =

1.162
1.135

$\mathbf{K}_{2,0.9}$ =

0.428	1.096
1.096	0.000

$\mathbf{P}_{2,0.9}$ =

1.951
1.096

$\mathbf{K}_{2,1}$ =

0.808	1.190
1.190	0.000

$\mathbf{P}_{2,1}$ =

2.806
1.190

Trimers

AB_2

$\mathbf{K}_{3,0.5}$ =

0.035	1.012	0.965
1.012	0.000	0.039
0.965	0.039	0.000

$\mathbf{P}_{3,0.5}$ =

2.047
1.051
1.004

$\mathbf{K}_{3,0.9}$ =

0.346	1.112	0.654
1.112	0.000	0.385
0.654	0.385	0.000

$\mathbf{P}_{3,0.9}$ =

2.458
1.497
1.039

$\mathbf{K}_{3,1}$ =

0.701	1.220	0.299
1.220	0.000	0.780
0.299	0.780	0.000

$\mathbf{P}_{3,1}$ =

2.922
2.000
1.078

AB_4

$\mathbf{K}_{3,0.5}$ =

0.061	1.016	0.951
1.016	0.000	0.053
0.951	0.053	0.000

$\mathbf{P}_{3,0.5}$ =

2.089
1.069
1.004

$\mathbf{K}_{3,0.9}$ =

0.392	1.097	0.687
1.097	0.000	0.337
0.687	0.337	0.000

$\mathbf{P}_{3,0.9}$ =

2.568
1.434
1.024

$\mathbf{K}_{3,1}$ =

0.758	1.194	0.388
1.194	0.000	0.657
0.388	0.657	0.000

$\mathbf{P}_{3,1}$ =

3.099
1.850
1.045

Tetramers

AB_2

$\mathbf{K}_{4,0.5}$

0.033	1.009	0.967	0.141
1.009	0.000	0.037	0.825
0.967	0.037	0.000	0.035
0.141	0.825	0.035	0.000

$\mathbf{P}_{4,0.5}$

2.183
1.871
1.039
1.001

$\mathbf{K}_{4,0.9}$

0.315	1.105	0.685	0.118
1.105	0.000	0.359	0.546
0.685	0.359	0.000	0.349
0.118	0.546	0.349	0.000

$\mathbf{P}_{4,0.9}$

2.538
2.010
1.393
1.014

$\mathbf{K}_{4,1.0}$

0.647	1.229	0.353	0.089
1.229	0.000	0.736	0.212
0.353	0.736	0.000	0.734
0.089	0.212	0.734	0.000

$\mathbf{P}_{4,1.0}$

2.965
2.177
1.823
1.035

AB_4

$\mathbf{K}_{4,0.5}$

0.057	1.015	0.959	0.188
1.015	0.000	0.046	0.772
0.959	0.046	0.000	0.041
0.188	0.772	0.041	0.000

$\mathbf{P}_{4,0.5}$

2.276
1.833
1.046
1.001

$\mathbf{K}_{4,0.9}$

0.361	1.099	0.742	0.148
1.099	0.000	0.291	0.604
0.742	0.291	0.000	0.257
0.148	0.604	0.257	0.000

$\mathbf{P}_{4,0.9}$

2.711
1.994
1.289
1.008

$\mathbf{K}_{4,1.0}$

0.729	1.190	0.479	0.103
1.190	0.000	0.587	0.398
0.479	0.687	0.000	0.514
0.103	0.398	0.514	0.000

$\mathbf{P}_{4,1.0}$

3.229
2.175
1.580
1.015

Hexamers

AB_2

$\mathbf{K}_{6,0.5}$

0.030	1.000	0.763	0.488	0.218	0.001
1.000	0.000	0.248	0.487	0.287	0.035
0.763	0.248	0.000	0.029	0.477	0.453
0.488	0.487	0.029	0.000	0.020	0.491
0.218	0.287	0.477	0.020	0.000	0.020
0.001	0.035	0.453	0.491	0.020	0.000

$\mathbf{P}_{6,0.5}$

2.529
2.057
1.969
1.515
1.021
1.000

$\mathbf{K}_{6,0.9}$

0.299	0.978	0.681	0.322	0.144	0.007
0.978	0.000	0.432	0.456	0.349	0.073
0.681	0.432	0.000	0.289	0.331	0.271
0.322	0.456	0.289	0.000	0.183	0.464
0.144	0.349	0.331	0.183	0.000	0.187
0.007	0.073	0.271	0.464	0.187	0.000

$\mathbf{P}_{6,0.9}$

2.732
2.289
2.004
1.714
1.194
1.002

$\mathbf{K}_{6,1.0}$

0.617	0.957	0.608	0.127	0.050	0.019
0.957	0.000	0.644	0.403	0.452	0.127
0.608	0.644	0.000	0.619	0.129	0.038
0.127	0.403	0.619	0.000	0.388	0.424
0.050	0.452	0.129	0.388	0.000	0.397
0.019	0.127	0.038	0.424	0.397	0.000

$\mathbf{P}_{6,1.0}$

2.994
2.582
2.037
1.962
1.415
1.005

AB_4

$\mathbf{K}_{6,0.5}$

0.058	0.994	0.717	0.624	0.313	0.002
0.994	0.004	0.304	0.344	0.344	0.102
0.717	0.304	0.000	0.041	0.326	0.528
0.624	0.344	0.041	0.000	0.018	0.349
0.313	0.344	0.326	0.010	0.000	0.019
0.002	0.102	0.528	0.349	0.019	0.000

$\mathbf{P}_{6,0.5}$

2.765
2.096
1.916
1.377
1.020
1.001

$\mathbf{K}_{6,0.9}$

0.333	0.981	0.655	0.466	0.261	0.011
0.981	0.013	0.456	0.364	0.376	0.110
0.655	0.456	0.000	0.215	0.269	0.376
0.466	0.364	0.215	0.000	0.098	0.403
0.261	0.376	0.269	0.098	0.000	0.101
0.011	0.110	0.376	0.403	0.101	0.000

$\mathbf{P}_{6,0.9}$

3.099
2.313
1.970
1.547
1.105
1.001

$\mathbf{K}_{6,1.0}$

0.663	0.968	0.629	0.260	0.186	0.025
0.968	0.033	0.609	0.403	0.432	0.123
0.629	0.609	0.000	0.423	0.202	0.173
0.260	0.403	0.423	0.000	0.098	0.403
0.186	0.432	0.202	0.189	0.000	0.192
0.025	0.123	0.173	0.403	0.192	0.000

$\mathbf{P}_{6,1.0}$

3.393
2.601
2.036
1.765
1.201
1.003

Decamers

AB_2

$\mathbf{K}_{10,0.93}$ (upper part only) and $\mathbf{K}_{10,1.00}$ (lower part only)

0.26	0.72	0.60	0.41	0.26	0.11	0.12	*0.18*	0.03	0.00
	0.00	0.40	0.46	0.32	0.16	0.20	0.26	0.17	0.01
0.58		0.00	0.32	0.27	0.29	0.12	0.16	0.13	0.03
0.66	0.00		0.00	0.28	0.29	0.07	0.12	0.10	0.01
0.53	0.41	0.00		0.00	0.24	0.32	0.07	0.19	0.05
0.43	0.56	0.31	0.00		0.00	0.23	0.12	0.20	0.31
0.14	0.48	0.33	0.27	0.00		0.00	0.10	0.17	0.35
0.04	0.25	0.26	0.27	0.37	0.00		0.00	0.03	0.22
0.02	0.15	0.22	0.08	0.26	0.38	0.00		0.00	0.03
0.02	0.23	0.26	0.09	0.08	0.10	0.24	0.00		0.00
0.00	0.20	0.22	0.09	0.08	0.22	0.13	0.07	0.00	
0.00	0.01	0.04	0.02	0.01	0.12	0.40	0.36	0.06	0.00

$\mathbf{P}_{10,0.93}$

2.934
2.688
2.305
2.056
2.000
1.947
1.671
1.255
1.003
1.000

$\mathbf{P}_{10,1.00}$

3.000
2.940
2.565
2.120
2.000
1.998
1.878
1.434
1.060
1.000

AB_4

$\mathbf{K}_{10,0.90}$ (upper part only) and $\mathbf{K}_{10,1.00}$ (lower part only)

0.27	0.72	0.65	0.47	0.26	0.19	*0.26*	0.22	0.04	0.00
	0.06	0.37	0.42	0.34	0.16	0.25	0.32	0.12	0.01
0.52		*0.01*	0.29	0.29	0.21	0.12	0.19	0.18	0.04
0.66	*0.11*		0.00	0.25	0.27	0.27	0.05	0.16	0.04
0.55	0.44	*0.00*$_4$		0.00	0.23	0.20	0.05	0.25	0.13
0.51	0.48	0.27	*0.00*$_4$		0.00	0.17	0.06	0.16	0.39
0.25	0.40	0.33	0.23	0.00		0.00	0.04	0.09	0.29
0.13	0.21	0.26	0.24	0.29	0.00		0.00	0.01	0.10
0.18	0.20	0.17	0.12	0.17	0.25	0.00		0.00	0.01
0.16	0.25	0.28	0.10	0.07	0.07	0.10	0.00		0.00
0.05	0.14	0.23	0.12	0.18	0.19	0.07	0.03	0.00	
0.00	0.02	0.05	0.04	0.07	0.29	0.36	0.16	0.02	0.00

$\mathbf{P}_{10,0.90}$

3.325
2.820
2.359
2.069
1.985
1.848
1.458
1.118
1.006
1.000

$\mathbf{P}_{10,1.00}$

3.523
3.010
2.585
2.124
2.001
1.931
1.617
1.196
1.018
1.000

Tetradecamers

AB_2

$\mathbf{K}_{14,0.93}$ (upper part only) and $\mathbf{K}_{14,1.00}$ (lower part only)

j: 1	2	3	4	5	6	7	8	9	10	11	12	13	14
0.25	0.63	*0.54*	0.44	0.31	0.17	0.12	0.06	0.04	0.05	0.09	0.05	0.00	0.00
	0.00	0.24	0.40	0.41	0.29	0.18	0.11	0.09	0.14	0.23	0.14	0.05	0.01
		0.00	0.19	*0.28*	*0.28*	0.23	0.16	0.11	0.16	*0.20*	*0.18*	0.04	0.01
0.57			0.00	0.18	0.23	0.20	0.15	0.12	0.06	0.13	0.13	0.06	0.01
0.61	0.00			0.00	0.22	0.20	0.15	0.12	0.00	0.04	0.09	0.04	0.00
0.33	*0.35*	0.00			0.00	0.22	0.21	0.17	0.06	0.05	0.08	0.03	0.00
0.33	0.41	0.22	0.00			0.00	*0.26*	0.20	0.13	0.03	0.13	0.10	0.02
0.31	0.46	0.32	0.17	0.00			0.00	*0.23*	*0.21*	0.05	0.12	*0.20*	0.08
0.15	0.39	*0.36*	0.22	0.16	0.00			0.00	0.18	0.02	0.04	*0.25*	0.26
0.08	0.22	0.31	0.21	0.17	0.18	0.00			0.00	0.07	0.03	*0.17*	0.38
0.03	0.12	*0.21*	*0.17*	*0.19*	*0.21*	*0.26*	0.00			0.00	0.03	0.06	0.19
0.01	0.09	0.15	0.15	0.09	0.13	0.25	*0.29*	0.00			0.00	0.01	0.06
0.01	0.09	0.12	0.12	0.05	0.10	0.18	*0.19*	0.24	0.00			0.00	0.00
0.00	0.11	*0.22*	0.18	0.08	0.07	0.04	0.07	0.12	0.16	0.00			0.00
0.00	0.10	*0.21*	0.23	0.13	0.03	0.05	0.09	0.05	0.06	0.06	0.00		
0.00	0.05	*0.08*	*0.14*	0.04	0.02	0.05	*0.11*	*0.28*	*0.14*	0.07	0.01	0.00	
0.00	0.00	0.01	0.02	0.00	0.00	0.00	0.06	0.14	0.38	0.27	0.12	0.00	0.00

AB_4

$\mathbf{K}_{14,0.89}$ (upper part only) and $\mathbf{K}_{14,1.00}$ (lower part only)

j: 1	2	3	4	5	6	7	8	9	10	11	12	13	14
0.27	0.62	*0.46*	0.46	0.42	0.21	0.10	0.11	0.18	0.26	0.15	0.03	0.00	0.00
	0.07	0.32	0.33	0.35	0.31	0.19	0.12	0.13	0.22	0.23	0.25	0.02	0.00
		0.01	0.22	0.28	*0.31*	0.24	0.13	0.10	0.17	*0.27*	0.21	0.05	0.00
0.51			0.00	0.18	0.22	0.24	0.14	0.06	0.05	0.18	0.23	*0.08*	0.00
0.60	*0.13*			0.00	0.14	0.21	0.17	0.08	0.03	0.05	0.11	*0.07*	0.02
0.33	*0.38*	*0.02*			0.00	0.22	0.23	0.11	0.02	0.03	0.11	*0.10*	0.01
0.34	0.31	0.30	0.00			0.00	0.18	0.19	0.06	0.02	0.11	*0.17*	0.08
0.44	0.40	0.25	0.21	0.00			0.00	0.20	0.13	0.01	0.05	*0.24*	0.23
0.26	0.33	*0.36*	0.20	0.13	0.00			0.00	0.08	0.04	0.01	*0.19*	0.34
0.10	0.22	0.29	0.25	0.15	0.22	0.00			0.00	0.02	0.01	0.07	0.23
0.06	0.14	0.19	0.19	0.17	0.16	0.25	0.00			0.00	0.00	0.01	0.07
0.14	0.08	0.13	0.10	0.08	0.16	0.20	0.19	0.00			0.00	0.00	0.01
0.24	0.14	0.13	0.08	0.03	0.06	0.06	0.14	0.14	0.00			0.00	0.00
0.12	0.17	*0.27*	0.21	0.06	0.01	0.03	0.03	0.05	0.07	0.00			0.00
0.04	0.09	0.18	0.27	0.16	0.06	0.07	0.08	0.03	0.02	0.01	0.00		
0.01	0.02	0.07	*0.12*	*0.09*	0.05	*0.13*	*0.20*	*0.22*	0.08	0.02	0.01	0.00	
0.00	0.00	0.01	0.01	0.02	0.01	0.03	0.19	0.31	0.29	0.12	0.02	0.00	0.00

Duodecamers

AB_2 $\mathbf{K}_{20,0.89}$ (upper part only) and $\mathbf{K}_{20,1.00}$ (lower part only)

j: 1	2	3	4	5	6	7	8	9	10	11	12	13	14	15	16	17	18	19	20
0.24	*0.61*	0.36	0.29	0.32	0.21	0.13	0.07	0.08	0.04	0.02	0.02	0.00	0.02	0.02	0.01	0.01	0.00	0.00	0.00
	0.00	0.21	0.25	0.31	*0.32*	0.30	0.21	0.17	0.12	0.08	0.04	0.06	0.04	0.11	*0.12*	0.05	0.01	0.00	0.00
		0.00	0.16	0.19	0.24	0.31	0.23	*0.23*	*0.14*	0.13	0.07	0.09	0.08	0.13	0.19	0.14	0.06	0.00	0.00
0.57			0.00	0.14	0.17	0.17	0.25	0.16	*0.14*	0.09	0.11	0.08	0.10	0.15	0.20	0.19	0.08	0.02	0.00
0.57	0.00			0.00	0.10	0.17	0.15	0.17	*0.11*	0.11	0.07	0.05	0.06	0.09	0.15	0.18	0.08	0.03	0.01
0.22	0.37	0.00			0.00	0.08	0.15	0.12	*0.16*	0.09	0.06	0.06	0.05	0.04	0.08	0.09	0.05	0.01	0.00
0.16	0.21	0.22	0.00			0.00	0.12	0.13	*0.15*	0.11	0.07	0.07	0.04	0.02	0.02	0.04	0.04	0.02	0.00
0.21	0.28	0.17	0.17	0.00			0.00	0.13	*0.11*	0.18	0.10	0.09	0.06	0.01	0.02	0.04	0.02	0.01	0.00
0.27	0.31	0.27	0.18	0.11	0.00			0.00	*0.15*	0.15	*0.21*	0.11	0.05	0.02	0.02	0.04	0.06	0.02	0.00
0.21	*0.40*	0.29	0.22	0.12	0.09	0.00			0.00	*0.18*	*0.14*	*0.16*	0.09	0.04	0.02	0.07	0.09	0.04	0.01
0.12	0.29	0.28	0.27	0.19	0.12	0.09	0.00			0.00	0.24	0.12	0.15	0.06	0.01	0.06	0.10	0.10	0.02
0.07	0.18	0.23	0.23	*0.24*	0.11	0.09	0.08	0.00			0.00	0.18	0.16	0.10	0.03	0.03	0.17	0.13	0.07
0.02	0.12	0.18	0.18	0.21	0.14	0.14	0.11	0.10	0.00			0.00	0.14	0.14	0.04	0.03	0.13	0.24	0.18
0.02	0.07	0.15	0.13	0.12	0.12	0.11	0.17	*0.18*	0.14	0.00			0.00	0.13	0.04	0.01	0.06	0.23	0.28
0.01	0.03	0.08	0.09	0.08	0.08	0.09	0.10	*0.20*	0.18	0.23	0.00			0.00	0.04	0.01	0.02	0.13	0.27
0.00	0.04	0.07	0.09	0.08	0.07	0.06	0.06	0.13	0.16	0.16	0.24	0.00			0.00	0.00	0.00	0.02	0.14
0.00	0.03	0.10	0.09	0.07	0.02	0.04	0.04	0.07	0.16	0.12	0.17	0.16	0.00			0.00	0.00	0.00	0.02
0.00	0.03	0.10	0.17	0.12	0.05	0.01	0.05	0.03	0.06	0.02	0.11	0.15	0.14	0.00			0.00	0.00	0.00
0.00	0.05	0.10	0.17	0.22	0.15	0.03	0.02	0.01	0.03	0.02	0.03	0.02	0.10	0.05	0.00			0.00	0.00
0.00	0.03	0.13	0.22	0.22	0.16	0.06	0.04	0.01	0.02	0.04	0.04	0.03	0.01	0.03	0.01	0.00			0.00
0.00	0.01	0.03	0.13	0.10	0.12	0.05	0.01	0.03	0.05	0.12	0.14	0.13	0.07	0.02	0.00	0.00	0.00		
0.00	0.00	0.00	0.03	0.02	0.03	0.01	0.01	0.01	0.02	0.06	0.10	0.24	0.22	0.16	0.08	0.01	0.00	0.00	
0.00	0.00	0.00	0.00	0.00	0.00	0.00	0.00	0.00	0.00	0.01	0.02	0.11	0.29	0.32	0.20	0.04	0.00	0.00	0.00

AB_4 $\mathbf{K}_{20,0.90}$ (upper part only) and $\mathbf{K}_{20,1.00}$ (lower part only)

j: 1	2	3	4	5	6	7	8	9	10	11	12	13	14	15	16	17	18	19	20
0.20	0.59	0.34	0.27	0.32	0.45	0.34	0.19	0.11	0.05	0.06	0.04	0.12	0.17	0.12	0.08	0.01	0.00	0.00	0.00
	0.09	0.33	0.20	0.23	0.26	*0.29*	0.21	0.14	0.08	0.05	0.04	0.11	0.17	0.19	0.08	0.03	0.01	0.00	0.00
		0.04	0.23	0.17	0.21	0.21	0.32	0.18	0.14	0.10	0.07	0.03	0.07	0.20	0.21	0.07	0.03	0.01	0.00
0.45			*0.01*	0.14	0.13	0.22	0.20	*0.24*	0.17	0.14	0.07	0.07	0.10	0.16	0.23	0.20	0.06	0.01	0.00
0.52	*0.13*			0.00	0.12	0.16	0.15	0.19	0.15	0.11	0.10	0.05	0.05	0.10	0.21	0.20	0.13	0.01	0.00
0.37	0.38	*0.03*			0.00	0.09	0.10	0.13	0.16	0.10	0.07	0.03	0.02	0.04	0.13	0.07	0.02	0.00	0.00
0.16	0.28	0.23	*0.02*			0.00	0.09	0.09	0.17	0.13	0.06	0.05	0.01	0.01	0.02	0.07	0.02	0.01	0.00
0.24	0.20	0.19	0.15	0.00			0.00	0.11	0.12	0.14	0.13	0.06	0.02	0.01	0.01	0.06	0.06	0.01	0.00
0.37	0.23	0.21	0.17	0.13	0.00			0.00	0.11	0.15	*0.17*	0.11	0.06	0.01	0.00	0.07	0.11	0.02	0.00
0.37	0.25	0.24	0.23	0.18	0.06	0.00			0.00	0.14	0.19	0.15	0.07	0.02	0.01	0.06	0.11	0.08	0.02
0.19	0.25	0.30	0.23	0.68	0.17	0.08	0.00			0.00	0.14	0.18	0.09	0.02	0.01	0.06	0.15	0.19	0.06
0.09	0.21	0.19	*0.28*	0.18	0.13	0.10	0.12	0.00			0.00	0.11	0.15	0.02	0.01	0.02	0.14	0.23	0.21
0.07	0.11	0.16	0.23	0.19	0.10	0.11	0.10	0.09	0.00			0.00	0.04	0.06	0.00	0.01	0.08	0.23	0.29
0.04	0.04	0.12	0.13	0.16	0.14	0.11	0.11	*0.17*	0.19	0.00			0.00	0.04	0.02	0.01	0.02	0.13	0.25
0.01	0.08	0.06	0.08	0.11	0.07	0.11	0.12	0.15	0.15	0.19	0.00			0.00	0.00	0.00	0.01	0.03	0.15
0.10	0.06	0.06	0.08	0.07	0.07	0.04	0.06	0.08	0.15	0.14	0.16	0.00			0.00	0.00	0.00	0.01	0.02
0.17	0.15	0.07	0.09	0.05	0.05	0.02	0.01	0.05	0.06	0.08	0.11	0.11	0.00			0.00	0.00	0.00	0.00
0.15	0.11	0.19	0.14	0.13	0.05	0.04	0.01	0.02	0.02	0.03	0.04	0.05	0.05	0.00			0.00	0.00	0.00
0.07	0.09	0.13	0.22	0.23	0.12	0.05	0.02	0.02	0.02	0.01	0.01	0.00	0.04	0.01	0.00			0.00	0.00
0.03	0.03	0.05	0.15	0.26	0.21	0.08	0.04	0.03	0.04	0.03	0.02	0.01	0.01	0.00	0.00	0.00			0.00
0.00	0.02	0.05	0.07	0.12	0.13	0.07	0.07	0.06	0.14	0.12	0.09	0.07	0.02	0.00	0.00	0.00	0.00		
0.00	0.00	0.01	0.01	0.04	0.02	0.02	0.01	0.04	0.06	0.17	0.19	0.27	0.12	0.02	0.04	0.00	0.00	0.00	
0.00	0.00	0.00	0.00	0.00	0.00	0.00	0.00	0.01	0.20	0.02	0.02	0.25	0.25	0.17	0.01	0.02	0.00	0.00	0.00

[a] The standard errors justify the number of significant figures given and are similar to those provided before.[17] The accurate intervals of p_a were 0.497 884, 0.928 628, and 0.999 966 for the $\mathbf{AB}_2$ system and 0.465 46, 0.896 60, and 0.999 74 for the $\mathbf{AB}_4$ system.

systems give just about the same results (it is likely that the accuracy of the simulation percentages is little better than the discrepancies we show). The $\mathbf{AB}_4$ system, in contrast, gives a much smaller proportion of these isomers, an exception being the two isomers that are highly branched and marked with an asterisk. There is, to compensate, a large proportion of new isomers, in which there is a node that has reacted four or even more times, but the fraction of each is quite small. From the value of $\langle \mathbf{P}_{6,1}[1] \rangle = 3.393$ we may conclude that up to 39% of the structural isomers contain a node that has four links, though a small proportion of an isomer with a node that has reacted five times may reduce that figure a little: we were able to find one looped isomer, whose node had used all five functional groups at the 0.9% level, and a second at the 0.8% level. These new isomers are grouped at the end of the section on hexamers, which is not exhaustive, for at least 42 forms might occur, more than twice the number possible for the $\mathbf{AB}_2$ case. As we do not identify the site of the **A** group on the trees, our proportions differ from those provided by ω_6 (of eq 10). Our simulation has provided the structures of 19 isomers that might occur in proportions greater than 1%. From the values of $\langle \mathbf{K}_{6,1}[1,1] \rangle = 0.663$ and $\langle \mathbf{K}_{6,1}[2,2] \rangle = 0.033$ we conclude that 69.6% of the isomers contains a loop, a larger proportion that we found for the $\mathbf{A}-N(-\mathbf{B})_2$ hexamers (61.7% from $\langle \mathbf{K}_{6,1}[1,1] \rangle$ alone).

We see in the mean Kirchhoff matrices and extent of reaction vectors of Scheme 1 for the systems the pattern of bonding that emerges for the two systems at the three stages of the reaction we have chosen. The $\langle \mathbf{P}_6[i] \rangle$ values for the $\mathbf{A}-N(-\mathbf{B})_2$ system suggest that at the halfway stage half the molecules are linear and about half have a branch (this follows from the element's values of [2.5, 2.0, 2.0, 1.5, 1.0, 1.0]), but ultimately on average there is one extra branch point, that in a cycle at the root of the branch. At the halfway stage also loops are a minor component from $\langle \mathbf{K}_{6,0.5}[1,1] \rangle$, and reading along the top row, N_1 is linked to the others with frequencies that decrease smoothly with i. As loops form that pattern is maintained for the hexamers in both systems, there being a small increase in the frequency with which the final node is linked to N_1, especially in the $\mathbf{AB}_4$ series. As the degree of branching develops during the reaction, the frequency with which nodes 4 and 5 are linked to N_1 decreases: the initial role of N_4 is to link N_1 or N_2 to N_6, or to be simply a pendent unit to those nodes, but ultimately its main role is to act as a link between N_3 and N_6. In the $\mathbf{A}-N(-\mathbf{B})_4$ system there is a similar role for N_4, modified by a possibility for it also to be pendant to the more highly reacted N_1.

We now turn to the representatives of the larger oligomers, the decamers, tetradecamers, and the duodecamers, whose Kirchhoff matrices are shown in Scheme 3 for the final two stages we have selected (when $p_a = 0.5$, these molecules have yet to form). For the $\mathbf{A}-N(-\mathbf{B})_2$ system we can see in $\mathbf{P}_{10,1.0}$ that at the end the elements are related by $\mathbf{P}_{10,1.0}[i] + \mathbf{P}_{10,1.0}[11 - i] = 4.000$: for every branch point there is one terminator (this is exactly so for $x = 20$). We may also conclude that none of the isomers have, on average, five branch points, 12% of the isomers have 4 branch points, 57% have three, 94% have two, and all have one—since the fraction containing a six-membered ring is negligible. (For the hexamers at the end, similar features are seen in $\mathbf{P}_{6,1.0}[i]$, but 0.5% of those molecules contain the six-membered ring.) Before the end, among the decamers, N_1 is linked to the other nodes with an increasing frequency as i rises, but the trend is reversed at N_8 for the $\mathbf{A}-N(-\mathbf{B})_2$ system and a N_7 for the $\mathbf{A}-N(-\mathbf{B})_4$ system, those nodes being required to terminate chains. At the end this trend is still the same for the for the $\mathbf{A}-N(-\mathbf{B})_4$ system, but for the other the downward trend only is found. Inspection of the matrices for the tetradecamers and the duodecamers reveals the same features, but the second maximum in the $\mathbf{A}-N(-\mathbf{B})_2$ case is much reduced even at the $p_a = 0.9$ stage, for it can only be found in molecules in which the primary node has reacted three times, and bears a unit side chain or *tail*. It is possible to recognize the role of any node in the half matrices we show, by first reading along a row and then—after the diagonal—down a column, or vice versa. For example, three roles are found for the third node of the tetradecamers in the $\mathbf{A}-N(-\mathbf{B})_2$ system: maxima being found at the first, the fifth and sixth, and 11th positions when $p_a = 0.9$ moving to the second, sixth, and 11th and 12th positions when the reaction is complete. The behavior is similar in the $\mathbf{A}-N(-\mathbf{B})_4$ system. In the $\mathbf{A}-N(-\mathbf{B})_2$ system before the end the eighth node is linked to the group of nodes N_6 to N_{10} (though not to itself), but at the end of the reaction it is linked significantly to a larger range, N_3 to N_{10}. The role of N_{13} changes as the reaction becomes completed, being linked to a group of nodes N_7 to N_{10}, and then to two groups, mainly N_8 to N_{10} but also to N_3 and N_4. This behavior is modified slightly in the $\mathbf{A}-N(-\mathbf{B})_4$ system too.

The calculations have provided matrices for the duodecamers that reveal patterns of bonding within the larger sets of structural isomers that may form, with values of $\langle \mathbf{K}_{20,1}[i,j] \rangle$ that are lower, as the links are shared over a larger number of residues when x rises. Thus, N_2 is most often linked to to N_1 (61%), to N_5 (32%), and to N_{16} (12%) when $p_a = 0.9$ in the $\mathbf{A}-N(-\mathbf{B})_2$ oligomers, but at the end the pattern is simpler, N_2 then most often linked to N_1 (57%), to N_3 (37%), and to N_7 (40%). For the dodecamers of the $\mathbf{A}-N(-\mathbf{B})_4$ system N_2 is most often linked to N_1 (59%), to N_7 (29%), and to N_{15} (19%) when $p_a = 0.9$, but at the end the pattern is again simpler, N_2 then being usualy linked to N_1 (52%) and to N_{14} (15%).

From the entries in the $\langle \mathbf{K}_{x,1}[i,i] \rangle$ positions of Scheme 3 we obtained the proportions of looped molecules at the end:[62] the values fall from 100% for the monomers to about 60% for the dodecamers, the proportion being slightly greater for the $\mathbf{A}-N(-\mathrm{B})_4$ system than for the $\mathbf{A}-N(-\mathbf{B})_2$ system (which is very much like the $\mathbf{A}-X-X-N(-\mathbf{B})_2$ system).[17] At earlier values of p_a we have found the values of total cycle content within each $x$mer: the values diminish in a similar fashion. For the $f = 2$ system, when $p_a = 0.93$ the fraction of molecules that contain a cycle falls from 65% to about 43% as x rises to 20; for the $f = 4$ system the corresponding fractions are 56% and 50%. At this value of p_a and even much earlier for the low x oligomes, the proportion of cycles that are loops ($m = 1$) is more sensitive to x than to p_a.[62] These figures reflect the natural tendency for the larger cycles to be found in the larger molecules, but the predominance of loops throughout emphasizes the importance, in our model, of allowing three-membered rings to form readily upon the lattice. (If we ban loops on account of ring strain, their role in limiting growth is taken by two-residue cycles.)[22] The model is

thus appropriate for real molecules in which the covalent bonds are rather flexible in their configurations[30,31]—though we might modify this feature by preventing lattice angles less than, e.g., $\pi/2$. Feast's experiments with fairly stiff molecules have shown that stiffness merely shifts the predominant cycles to larger m.[33]

For both systems and for every oligomer whose matrices are shown it is clear that during the final stages of the reaction there is a considerable change in the loop content measured by $\langle \mathbf{K}[1,1] \rangle$, $\langle \mathbf{K}[2,2] \rangle$, etc. Thus, for the final 10% change in p_a the decamer loop content rises from 26% to 58% for the $\mathbf{A}-N(-\mathbf{B})_2$ system, and from 34% to 64% for the $\mathbf{A}-N(-\mathbf{B})_4$ system. These changes are too large to be solely the consequence of the **A** group at the root of the tree reacting intramolecularly, but must reflect the production of new decamers by the growth of lower oligomers that already contain a loop, and the removal of other decamers by reactions. This is another aspect of the competition between growth and cyclization.

The plots of $\langle \mathbf{P}_{x,p}[i] \rangle$ against i of Figure 9a show that among the larger isomers of the $\mathbf{A}-N(-\mathbf{B})_2$ system the mean value of 2.00 is adopted at the end of the reaction by several nodes on each side of $x/2$, and that these chain extenders are just about matched by an equal number of branch points and chain ends (As we have found before,[17] the branch points:extenders:ends ratios are quite close to the proportion of 1:2:1, a result in agreement with one experimental global measurement[33]). A detailed inspection of the **P** vectors finds that, starting from the trimers, within which each type of residue may first be found, and then proceeding to higher oligomers, more precise ratios are ($x = 3$) 0.92:1.16:0.92; ($x = 4$) 1.02:1.96:1.02; ($x = 6$) 1.08:1.85:1.08; ($x = 10$) 1.05:1.91:01.05; ($x = 14$) 0.96:2.08:0.96; ($x = 20$) 1.01:1.98:1.01; the geometric mean of all even ones is 1.02:1.95:1.02. At the earlier stage of the reaction the proportion of branch points is smaller, and the plateaux in Figure 9a are found centered at slightly lower regions of i than $x/2$.

For the $\mathbf{A}-N(-\mathbf{B})_4$ system, the plots at the end of the polymerization show in Figure 9b, even for the trimers, a node with an $\langle \mathbf{P}_{x,1}[1] \rangle$ value greater than 3.000; on average for the decamers and for the tetradecamers there are two such nodes, and for the duodecamers there are three. For each of the extra branches allowed by raising f from 2 to 4 there is a corresponding increase in the proportion of nodes with $\langle \mathbf{P}_{x,1}[i] \rangle$ close to 1.000. Thus, the curves of Figure 9b are not centrosymmetric. With much higher oligomers than those reported here we might expect a plateau region at about $\langle \mathbf{P}_{x,1}[i] \rangle = 3.000$: it is incipient for the duodecamers, but a third plateau has not developed at $\langle \mathbf{P}_{20,1}[i] \rangle = 4$ by the time the polymerization ceases. If the same calculation is performed on the decamers of the $\mathbf{A}-N(-\mathbf{B})_4$ system, we obtain a ratio of 0.25:1.05:1.40:1.30 for nodes that have reacted more than three times, three times, twice, and just once (from the $\mathbf{P}[i]$ we cannot discover whether any nodes have reacted more than four times, and we have neglected that possibility). The gap between the lines for, e.g., the tetradecamer at $p_a = 0.9$ and 1.0 reflects the manner in which the cycle formation, the production of more highly branched forms from lower oligomers, and the reaction of more extended forms to give higher oligomers influences the distribution of extra extent of reaction of the ordered nodes. Nodes 3 and 4 and nodes 10 and 11 appear to participate about equally in these latter reactions; in the more extended $\mathbf{A}-X-X-N(-\mathbf{B})_2$ form, the differences instead were most marked in the low i region,[17] that is, within the core of the molecule.

The values of the elements in the **P** vectors of the oligomers in the $\mathbf{AB}_4$ series indicate how frequently a residue has reacted more than three times. For the trimers at the end of the reaction $\langle \mathbf{P}_{3,1}[1] \rangle$ is 3.099, so we may conclude that at least 9.9% of the residues contain an isomer in which the prime node has reacted four times: this must reflect the proportion of the structural isomer E; in fact, since $\langle \mathbf{P}_{3,1}[3] \rangle = 1.045$, and there are 4.5% of the three-ringed isomers present, we may conclude that E is as much as 14.4% (as is indeed the case: see Table 3). Among the tetramers the value of $\langle \mathbf{P}_{4,1}[1] \rangle = 3.229(\pm 0.012)$ indicates that 23% of the isomers contain an node that has reacted four times (isomers D or K) or a double proportion of the isomer K, which has a node that has reacted five times. Among the $\mathbf{AB}_4$ hexamers we may see that up to 39% of the isomers have a node that has reacted four times (or include a smaller fraction with a five times reacted node), and as we pass through the decamers, and the tetradecamers to the duodecamers, this proportion rises from 52% through 83% to 112%: then nearly every molecule contains a node that has reacted more than three times, with 4.8% containing three such nodes, 25% two, and 83% one. From the manner in which $\mathbf{K}[4,4]$ values are nonzero, it appears that of the 4.8% proportion of these larger molecules with at least three nodes that have reacted more than three times only 1.5% have a loop, for $x = 20$, so larger cycles are found in 3.3% of the cases.

These statistical ideas on the structures of the hyperbranched molecules resemble the sequence information provided for linear copolymers by high field NMR, when diad, triad, tetrad, etc. sequences are recognized, and models of reaction mechanisms are employed and tested.[64,65] For hyperbranched molecules such information may be obtained from the ^{13}C NMR spectrum only if the links between the atoms at the node have just a few bonds (say three for a sensitivity to the γ-gauche effect).[64−66] In a related system, oligomers of glycerol with succinic acid, some such sensitivity has been found in the ^{13}C NMR spectrum over distances of seven bonds,[66,67] but generally it may be possible to measure only the proportion of once-, twice-, and thrice-reacted residues.[33] Our models' predictions might be tested for flexible systems[29−31] in which the oligomers of Tables 3 and 4 predominate by coupling NMR to GPC, to reveal how critical is the coarse-grained nature of our lattice and our omission of first shell substitution effects.

(H) Fractal Characteristics.[10,68] We offer the following test of the fractal characteristics of the hyperbranched molecules, by comparing the entries on the final row of the mean $\mathbf{K}_{10,1}$ matrix with the averages of pairs of entries for the final *two* rows of $\langle \mathbf{K}_{20,1} \rangle$. For the $\mathbf{AB}_2$ system, these are (as %): (0,0) (1,1) (3,4) (1,2) (3,1) (10,12) (43,40) (38,36) (2,6) (0,0), and for the $\mathbf{AB}_4$ system: (0,0) (1,2) (3,5) (2,4) (15,7) (20,29) (44,36) (12,16) (1,4) (0,0). In each case the $\langle \mathbf{K}_{10,1} \rangle$ elements and the averaged values for the duodecamers rise and fall together, the values within a pair scarcely differing by more than a few %, which is the order of the errors: each have a minor maximum at $i/x = 0.3$ when the residues are linked to a branch point, and a major maximum at $i/x = 0.7$ (where the residues are linked to

spacers). The main difference between the pairs selected for the $\mathbf{AB}_4$ systems lies in the distributions near the second maximum, which is slightly more peaked for the larger oligomer. A further test is provided by the form of the $\langle \mathbf{P}[i] \rangle$ plots of Figure 9: at the end of the polymerization it appears that if the curves were replotted against i/x, they would tend to coincide. A limit to the scale of this apparent self-similar behavior is provided by the values of $\langle m \rangle$, which do not scale with x, as demonstrated by the values of $\mathbf{K}_{x,1}[1,1]$ which fell by a factor of 2 as x rose to 20 beyond, and by a comparison of the values of γ_1 (>2.7) with χ_1 (≤1.5). The mean size of the cycles is much smaller than the mean size of the molecules, and their distribution functions fall off much more sharply. Thus, the intrinsic fractal nature of the growth process itself—in the absence of cycle formation molecules become, and are self-similar to, their branches[1,10]—which even in the cyclized forms leads to some similarities within the smoothed **K** matrices and **P** vectors that describe the mean structures of the isomers formed in this simulation that includes cycle formation, is itself frustrated overall by the creation of a higher cutoff to the range of molecular weights created by the formation of cycles,[68] as Figure 2 shows.

Conclusions

The step growth reactions of flexible and moving $\mathbf{A}-N(-\mathbf{B})_f$ ($f = 2$ and 4) monomers have been performed upon a 26-choice lattice in three dimensions, with a model that is strong, in the sence that there is no parameter to adjust to vary ring occurrence. Growth is shown to be limited by the formation of cycles. For the first system the value of $\langle m \rangle_n$, the mean size of the cycles, has been found to be 1.65 and for the second system a slightly smaller value of 1.39 was obtained. The larger f the greater the ease with which the randomly branching system finds a route back to the **A** group at the root of the Cayley tree. Once that has happened, fractal growth by the molecule is terminated, for it no longer has the capacity to become a branch on another molecule. The product graph may then grow only by reactions of its **B** groups. By this process all measures of mean molecule size and the polydispersities are made finite, a reduction enhanced by doubling f, and which is conversly less severe for the more extended $\mathbf{A}-X-X-N(-\mathbf{B})_2$ monomer examined on the same lattice elsewhere.[17]

For the present and the other $\mathbf{AB}_2$ system the incidence of rings of size m follows a dual power function $R_m = C_o\, p_a^{\,m}\, m^{-\gamma_1}$, with γ_1 very close to e. The number and weight distributions of oligomers follow the Flory expression[1] to begin with, but as the reaction proceeds, and cycles accumulate, the expedient of replacing p_a with p_e (which omits the reactions that close cycles) fails, and when $p_a = 1.00$ power functions are again obtained: $N_x = N_{x,1} x^{-\chi_n}$, with $\chi_n = 1.5$. (The expedient works at all times when p_e is used in the Carothers function for $\langle x \rangle_n$.) When the reaction is complete, neither this power law, nor that for the distribution of cycles can be extended to very large values of x or m, for that would imply that the total weight in the system, $\sum N_{x,1} x^{-0.50} = N_{x,1}\zeta(0.50)$, and also $\langle m \rangle_{w,oo}$ ($\propto \sum m^{-0.718} = \zeta(0.718)$) be infinitely large; instead both x and m series must eventually decay more quickly than implied by the initial trends, so that their sums are finite. This changeover may happen because the cycle formation is enhanced in large oligomers, by other molecules tending to be excluded from the neighborhood of the **A** group at the root of large tree. This (anti-mean-field) behavior, that is a natural feature of our lattice model, appears to be general for the flexible $\mathbf{AB}_2$ system, for it was also found also for a representation in which the node was spaced from the **A** group by two extra beads:[17] $\mathbf{A}-\{-X-\}_g-N(-\mathbf{B})_2$, $g = 2$. The values of $\gamma_1 = e$ (apparently) and of $\chi_n = 1.50$ are independent of the manner in which the flexible $\mathbf{AB}_2$ monomer is mapped onto the lattice, but the prefactors in the power functions and quantities such as $\langle x \rangle_n$ are sensitive to this mapping.

From the Monte Carlo study of the $\mathbf{A}-N(-\mathbf{B})_4$ system, in contrast, within the range of m explored we found the log−log plots of R_m vs p_a to be curved, initial slopes steepening a little as each variable rose. The ring numbers follow the same general trend as before, $\boldsymbol{R}_m = C_o\, p_a^{\,m}\, m^{-\gamma_1}$ as far as the dependence upon p_a is concerned for low values of m, but even at the end of the reaction the value of γ_1 rises a little, from 2.77 for the first two points, that cover most of the cycles, up to 2.97(±0.02) for the first 10 values of m. That for the $\mathbf{A}-N(-\mathbf{B})_4$ system $\gamma_1 > e$ is another indication that cyclizations are easier as f rises. The N_x plots on the log−log scale are linear until $x > 12$. The initial slope is less than in the $\mathbf{A}-N(-\mathbf{B})_2$ system, χ_n increasing from 1.29_0 for the first two points, to 1.36(±0.01) for the first 10, and to 1.40(±0.01) for the first 20. The lower value we attribute to the greater ease with which branches form in these oligomers, and the curvature points to the development of the extra mechanism—previously postulated for the $\mathbf{A}-N(-\mathbf{B})_2$ system—of enhanced cyclization in the larger fractals promoted by the **A** group being screened from other molecules.

Depending upon the value of f and the manner in which the monomer is mapped upon the lattice, between 10 and 20% of the residues are consumed in cycle formation. Deviations from the Flory pattern are greater the greater the value of f, and the smaller the spacing between the **A** and the **B** groups. An enhancement of molecular weight and a postponement of the transition from the Flory behavior might be effected by greatly enhancing g and so reducing the importance of the intramolecular reaction in a flexible macromomomer: $\mathbf{A}-(-X-)_g-N(-\mathbf{B})_2$. Stiffness within the residue and at the N-**A**−**B**-N bonds might also have this effect, and could be included by preventing bond angles less than 90°. Such issues, which are well represented by the rotation isomeric state approximation, are less well included in this fluctuating bond model for a particular monomer, but it has indicated strongly the pattern of the reaction and so has provided a framework for such more delicate work.

This Monte Carlo simulation provides the proportions of the main structural isomers at each stage of the reaction. We have predicted how these change during the polymerization by presenting three sets of mole fractions of all the isomers of the oligomers up to $x = 4$ as well as for the predominant hexamers, as examples of the higher oligomers. For several degrees of polymerization, x, having ordered the nodes with a scheme of priority values, we also obtained mean extent of reaction vectors and mean connectivity or Kirchhoff matrices, and have examined these to show how they describe the evolution of the reaction. Some small differences from the $\mathbf{A}-X-X-N(-\mathbf{B})_2$ case[17] are noted in Scheme 2 among the hexamer populations, so it may be seen that

Table 5. The Pattern of the Final Products: Structures of the AB_2 and AB_4 Oligomers and Their Number Fractions as Functions of Degree of Polymerization, *x*, and Cycle Size, *m*[a]

	$x = 1$	$x = 2$	$x = 3$	$x = 4$	$x = 5$
$\mathbf{AB_2}$:	(40.5%)[b]	(13.7%)	(7.8%)	(4.9%)	(3.8%)
$\mathit{AB_4}$:	*(37.2%)*[b]	*(15.2%)*	*(8.5%)*	*(5.7%)*	*(4.2%)*
$m = 1$	CN-	CN-N-	CN-N-N-	CN-N-N-N-	CN-N-N-N-N-
				CN-N-N-	CN-N-N-N-
				N-	-N-
(78.6%)[c]					CN-N-N-N-
					N-
(81.5%)					-N-
					CN-N-N-N-
					-N-
			-N-N-N-	-N-N-N-N-	-N-N-N-N-N-
					-N-N-N-N-N-
					-N-N-N-N-
					-N-
				-N-N-N-	-N-N-N-N-
				-N-	-N-
$m = 2$		-N=N-	-N=N-N-	-N=N-N-N-	-N=N-N-N-N-
				-N-N=N-N-	-N-N=N-N-N-
(12.6%)					-N=N-N-N-
(13.1%)					-N-
				-N=N-N-	-N=N-N-N-
				-N-	-N-
					-N-N=N-N-
					-N-
$m = 3$			-N-N-	-N-N-N-	-N-N-N-N-
			N	N	N
(4.2%)					-N-N-N-N-
					N
(3.4%)					-N-N-N-
					-N-N-
$m = 4$				-N-N-	-N-N-N-
(1.9%)					
(1.3%)				-N-N-	-N-N-
$m = 5$					-N-N-N-
(0.9%) (0.9%)					-N-N-

[a] The structures shown in bold type are shared by both systems, but those peculiar to the AB_4 system are shown in italics. The free valencies (−) indicate the scope for further reactions at B groups but omits the two extra valencies of those AB_4 molecules shown in bold type. [b] From the records and N_e/N_o. [c] From the C_m values of Table 1 and N_e/N_o.

the structure of the products is somewhat sensitive to the way the flexible residue is mapped onto the lattice.

Table 5 summarizes the pattern for the major components present at the end of the reactions, to show that the pattern of the structural isomers in the $\mathbf{AB}_4$ system is more complex than in the $\mathbf{AB}_2$ system. In the former each residue might react up to five times, though the actual proportion of such is rather small, as they can form only when the first groups have been consumed. The table is almost complete as far as the cycles are concerned, for only 1.5 to 2% of the molecules have larger cycles, but is less so for the sizes of the species, for just more than 29% ($f = 2$ or 4) of the molecules are to be found with higher values of *x*, a proportion which is however smaller than in the $\mathbf{A}-X-X-N(-\mathbf{B})_2$ system.[17] None of these graph structures is provided by the earlier Flory theory. In the table there are 22 isomers common to both systems ($f = 2$ and 4), and an extra 12 peculiar to the latter. Among the isomers containing a loop ($m = 1$), there are 8 common forms and 8 more of the $\mathbf{AB}_4$ system, but the proportion of more-branched forms falls as *m* rises. In comparison to the scope of further reaction for the molecules of the $\mathbf{AB}_4$ series of oligomers, that of the $\mathbf{AB}_2$ oligomers is much smaller, for each node has at most two spare valencies. Less than a quarter of the $\mathbf{AB}_4$ oligomers have nodes that have reacted four or more times.

Some of the characteristics of the molecules have a fractal nature, but overall the development of a large range of sizes from that type of growth is frustrated by the formation of cycles which inevitably occurrs when each of the randomly branching walks upon the lattice happen by chance to return and react with the **A** group at the root of the tree.

Acknowledgment. C.R.H. thanks DENI for a CAST studentship, supported by Courtaulds Coatings, and R.A.W.M. thanks the EPSRC for a Fellowship. We record the help of K. Seddon, T. Evans, D. McKay, H. Kenny, D. Armitage, and Billand Douglas.

References and Notes

(1) Flory, P. J. *Principles of Polymer Chemistry*; Cornell University Press: Ithaca, N. Y. 1953 (Chapter 9); *J. Am. Chem. Soc.* **1952**, *74*, 2718.
(2) Flory, P. J. *J. Phys. Chem*. **1942**, *46*, 132.
(3) Turner, S. R.; Voit, B. I.; Mourney, T. H. *Macromolecules* **1993**, *26*, 4617.
(4) Malmstrom, E.; Hult, A. *Macromolecules* **1996**, *29*, 1222.
(5) Beginn, U.; Drohmann, C.; Muller, M. *Macromolecules* **1997**, *30*, 4112.
(6) Yan, D.; Muller, A. H. E.; Matyjaszewski, K. *Macromolecules* **1997**, *30*, 7024.
(7) Stockmayer, W. H. *J. Chem. Phys.* **1943**, *11*, 219.
(8) Miller, D. R.; Macosco, C. W. *Macromolecules* **1978**, *11*, 656.
(9) Dušek, K.; Gordon, M.; Ross-Murphy, S. B. *Macromolecules* **1978**, *11*, 236.
(10) Mandelbrot, B. B. *The Fractal Geometry of Nature*; Freeman: Oxford, England, 1982.
(11) Muller, A. H. E.; Yan, D.; Wucklow, M. *Macromolecules* **1997**, *30*, 7015.
(12) Fréchet, J. M. J.; Henmi, M.; Gitsov, I.; Aoshima, G.; Leduc, M. R.; Grubbs, R. B. *Science* **1995**, *269*, 1080.
(13) Fawcett, A. H.; McBride, F. V.; Rutherford, J. *Macromolecules* **1989**, *22*, 4536.
(14) Fawcett, A. H.; Mee, R. A. W.; McBride, F. V. *Macromolecules* **1995**, *28*, 1481.
(15) Fawcett, A. H.; McBride, F. V.; Mee, R. A. W. *Macromol. Chem. Theory Simul.* **1993**, *2*, 91.
(16) Fawcett, A. H.; McBride, F. V.; Mee, R. A. W. *Macromol. Symp.* **1994**, *81*, 161.
(17) Cameron, C.; Fawcett, A. H.; Hetherington, C.; Mee, R. A. W.; McBride, F. V. *J. Chem. Phys.* **1998**, *108*, 8235.
(18) Wall, F. T.; Erpenbeck, J. J. *J. Chem. Phys.* **1959**, *30*, 634.
(19) De Gennes, P. G. *Scaling Concepts in Polymer Physics*; Cornell University Press: Ithaca, NY, 1979.
(20) Hammersley, T. M.; Morton, K. W. *J. R. Stat. Soc. B*. **1954**, *16*, 23.
(21) Fawcett, A. H.; McBride, F. V.; McKay, D.; Mee, R. A. W. Work in progress.
(22) Johan, F. G. A.; Janson, J.; de Brabander-van den Berg; E. M. M.; Meijer, E. W. *Science* **1995**, *266*, 1266.

(23) Pólya, G. *Acta Math*. **1937**, *68*, 145.
(24) Read, R. C. In *Graph Connections*; Beineke, L. W., Wilson, R. J., Eds.; Oxford Science Publications, Clarendon Press: Oxford, England, 1997; p 13.
(25) Temple, W. B. *Makromol. Chem*. **1972**, *160*, 277.
(26) Dušek, K. *Recl. Trav. Chim. Pays-Bas* **1991**, *110*, 507.
(27) Fawcett, A. H.; Mee, R. A. W.; McBride, F. V. *J. Chem. Phys*. **1996**, *104*, 1743.
(28) Cameron, C.; Fawcett, A. H.; Hetherington, C.; Mee, R. A. W.; McBride, F. V. *ACS Polym. Prepr*. **1997**, *38* (1), 35.
(29) Mathias, L. J. Personal communication, Oct 20, 1997.
(30) Mathias, L. J.; Carothers, T. W.; Bozen, R. *ACS Polym. Prepr*. **1991**, *32* (1), 82.
(31) Miravet, J.; Frechet, J. M. *Macromolecules* **1998**, *31*, 3461.
(32) Simon, P. F. W. Diplomatarbeit, Mainz University, 1996; cited by ref 6.
(33) Feast, W. J.; Keeney, A. J.; Kenwright, A. M. Parker, D. *Chem. Commun*. **1997**, 1749.
(34) Kim, C.; Chang, Y.; Kim, J. S. *Macromolecules* **1996**, *29*, 6353.
(35) Fitzgerald, J. A.; Irwin, R. S. In *High Value Polymers*; Fawcett, A. H., Ed.; *Royal Society of Chemistry*; Cambridge, England, 1991.
(36) Tomalia, D. A.; Hedstrand, D. M.; Wilson, L. R. Dendritic Polymers. In *Concise Encyclopedia of Polymer Science and Engineering*; Kroschwitz, J.; Ed.; Wiley: Chichester, England, 1990; p 251.
(37) Newkome, G. R. *J. Heterocycl. Chem*. **1996**, *33*, 1445. Newcome, G. R.; Morefield, C. N.; Vogtle, F. *Dendritic Molecules*; VCH: Weinheim, Germany, 1996. Hawker, C. J. *Adv. Polym. Sci*. **1999**, *146*, 113.
(38) Holter, D.; Frey, H. *Acta Polym*. **1997**, *48*, 298.
(39) Lach, C.; Frey, H. *Macromolecules* **1998**, *31*, 2381.
(40) Rennard, S.; Davis, N. *ACS Div. Polym. Mater.: Sci. Eng*. **1997**, *77*, 63.
(41) Brender, C. *J. Chem. Phys*. **1977**, *67*, 1785. Gurler, M. T.; Crabb, C. C.; Dahlin, M.; Kovac, J. M. *Macromolecules* **1983**, *16*, 398.
(42) Carmesin, I.; Kremer, K. *Macromolecules* **1988**, *21*, 2819.
(43) Iwata, K. *Macromolecules* **1985**, *18*, 116.
(44) Werner, A.; Muller, M.; Schmid, F.; Binder, K. *J. Chem. Phys*. **1999**, *110*, 1221.
(45) Flory, P. J. *Statistical Mechanics of Chain Molecules*; Interscience: New York, 1969.
(46) Rehahn, M.; Mattice, W. L.; Suter, U. W. *Adv. Polym. Sci*. **1997**, *131/132*, 1.
(47) Jo, W. H.; Kim, J. G.; Jang, S. S.; Yonk, J. H.; Lea, S. C. *Macromolecules* **1999**, *32*, 1679.
(48) An investigation of the behavior of the molecule initialy placed within a sea of $\mathbf{A}_2$ dimers in two dimensions obtained the correlation times of a $\boldsymbol{Q}$ orientation function.[49] Before the simulation started in three dimensions we attempted to move the beads for 5 ($f = 2$) or 10 ($f = 4$) of the longest of these correlation times.
(49) Hetherington, C. R. Thesis, Queen's University, Belfast, Northern Ireland, 1998.
(50) Binder, K. *Monte Carlo Methods in Statistical Physics*; Binder, K., Ed.; Springer-Verlag: Berlin, 1979.
(51) Fawcett, A. H. Computer Applications, *In Macromolecular Chemistry, Specialist Periodical Reports*; Jenkins, A. D., Kennedy, J. F., Eds.; Royal Society of Chemistry: London, 1984; p 387.
(52) Verdier, P. G.; Stockmayer, W. H. *J. Chem. Phys*. **1962**, *36*, 227.
(53) Romiszowski, P.; Stockmayer, W. H. *J. Chem. Phys*. **1984**, *80*, 485.
(54) Lee, T. U.; Jang, S. S.; Yang, J. S.; Jo, W. H. *Proc. ACS Div. Polym. Mater.: Sci. Eng*. **1999**, *80*, 163.
(55) Cameron, C.; Fawcett, A. H.; Hetherington, C.; Mee, R. A. W.; McBride, F. V. *Chem. Commun*. **1997**, 1801.
(56) Volberg, J. J. *Prediction Analysis*; Van Nostrand: London, 1967.
(57) Jacobsen, H.; Stockmayer, W. H. *J. Chem. Phys*. **1950**, *18*, 1600.
(58) Truesdall, C. A. *Anal. Math*. **1945**, *46*, 144,.
(59) *Encyclopedia of Mathematics*; Kinogradov, I. M., Ed.; Reidel: Lancaster, England, 1988; Vol. 1, A-B.
(60) Jeffreys, H.; Swires, B. *Methods of Mathematical Physics*, 3rd ed.; Cambridge University Press: Cambridge, England, 1956.
(61) Beineke, L. W., Wilson, R. J., Eds. *Graph Connections*; Oxford Science Publications: Oxford, England, 1997.
(62) Wilson, R. J. *Introduction to Graph Theory*, 4th ed.; Longman: Harlow, England, 1996.
(63) The values of x, and the percentage of loops in the $\mathbf{AB}_2$ and $\mathbf{AB}_4$ systems at the end of the reactions were as follows: *1*, 100%, 100%; *2*, 74.7(±0.6)%, 80.8(±0.8)%; *3*, 70.1(±1.3)%, 76-(±2.3)%; *4*, 65(±1)%, 73(±2)%; *6*, 61.7(±1.5)%, 69.6(±1.5)%; *10*, 58(±2)%, 64(±2)%; *14*, 57(±2)%, 66(±4)%, *20*, 57(±3)%, 63(±3)%. Then all the molecules contained a cycle. When p_a was about 0.9, the percentages of loops and of all cycles in the $\mathbf{AB}_2$ and $\mathbf{AB}_4$ systems at selected values of x were as follows: *1*, 65%, 65%; 56%, 56%; *2*, 40%, 54%; 43%, 52%; *3*, 35%, 50%; 39%, 52%; *4*, 32%, 48%; 36%, 50%; *6*, 30%, 47%; 33%, 52%; *10*, 26%, 43%; 34%, 49%; *14*, 25%, 43%; 34%, 50%; *20*, 24%, 45%; 34%, 51%.
(64) Bovey, F. A. *Chain Structure and Conformation of Macromolecules*; Academic Press: London, 1982.
(65) Koenig, J. L. *Chemical Microstructure of Polymer Chains*; John Wiley & Sons: Chichester, England, 1980.
(66) (a) Tonelli, A. E.; (b) Fawcett, A. H.; Hamilton, J. G.; Rooney, J. J. In *Polymer Spectroscopy*; Fawcett, A. H., Ed.; John Wiley & Sons: Chichester, England, 1996.
(67) Fawcett, A. H.; Hania, M.; Lo, K.-W.; Patty, A. *J. Polym. Sci., A.: Polym. Chem*. **1994**, *32*, 815.
(68) Avnir, D.; Biham, O.; Lidar, D.; Malcai, O. *Science* **1998**, *279*, 39.

MA9916032